EMBEDDED CRACK PLATE SPECIMEN TO FIND INTERLAMINAR FRACTURE TOUGHNESS

A Thesis Submitted
in Partial Fulfillment of the Requirements
for the Degree of

MASTER OF TECHNOLOGY

By

VIMAL KUMAR JAISWAL

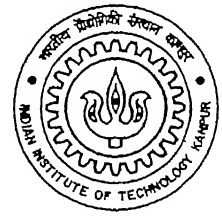

to the

Department of Mechanical Engineering

Indian Institute of Technology Kanpur

March, 2000

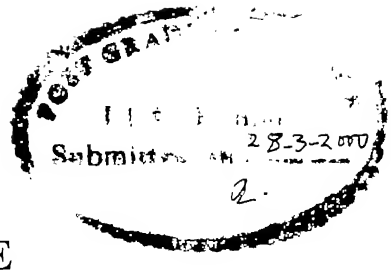

CERTIFICATE

It is certified that the work contained in the thesis entitled **"Embedded Crack Plate Specimen to find Interlaminar Fracture Toughness"**, by **Vimal Kumar Jaiswal**, has been carried out under my supervision and this work has not been submitted elsewhere for a degree.

P Kumar

March, 2000

(Dr.Prashant Kumar)
(Professor and Head)
Dept. of Mechanical Engineering
Indian Institute of Technology
Kanpur-208016

ACKNOWLEDGEMENTS

I wish to express my deep sense of gratitude and indebtedness to Prof. Prashant Kumar for his invaluable guidance, constructive suggestions and detailed instructions throughout this work inspite of his hectic schedule.

I express my sincere thanks to Prof. N. N. Kishore for his constant helps on many steps specially in installing CSA/NASTRAN on new P.C. and providing guidance and suggestions in FEM throughout the work. I also wish to thank Dr. Shenoy and Prof. P. M. Dixit for their invaluable suggestions.

Mr. Anurag Goal & Mr. Ramchandra Tiwari deserve special thanks who were constantly involved with me in preparing the specimens and helping me whole heartily. I can't forget Mr. B.K.Jain of ACMS who was always ready with me to do the experiments. I would like to thank Mr. Diwakar, Mr. B.D. Pandey, and Mr. Pankaj for their kind co-operation throughout the work.

It gives me immense pleasure to recall my association with Kamalesh Bhatt, Manish Pandey, Padamja, Himanshu, Arjun, & Sharad who made my stay at IITK, a pleasant memory.

In the last, I can't forget my association with all Gorakhpuriya friends of my wing specially Sudhir, Satyaveer, Anant, Om Prakash, Ram Kumar & Ravindra who made my life comfortable and enjoyable.

Vimal

ABSTRACT

Interlaminar toughness is determined through an experimental-numerical technique by employing a FRP Embedded Crack Plate (ECP) specimen. The embedded crack is circular to start with and is located at the midplane of the specimen. The specimen is pulled at the centre in tensile testing machine and embedded crack is allowed to grow. At regular interval the machine is stopped to mark the crack front. The Load vs. Deflection is monitored during the experimentation.

A Finite Element technique is developed and applied to process the experimental results to determine Interlaminar Fracture Toughness (G_{Ic}) using Virtual Crack Closure Integral (VCCI) technique. Three kinds of ECP specimens are used to determine G_{Ic} of configurations, (i) $[0/90]_{8s}$ glass fiber/epoxy laminate, (ii) $[0/+45/-45/90/90/-45/+45/0]_{2s}$ glass fabric/epoxy laminate, and (iii) $[0]_{32}$ glass fabric/epoxy laminate. The interlaminar toughness determined through ECP specimen is compared with interlaminar toughness found through the conventional DCB specimens.

CONTENTS

LIST OF FIGURES

LIST OF TABLES

CHAPTER-1

INTRODUCTION

1.1 INTRODUCTION

Fiber composite is a material, which consists of polymer reinforced with fibers of glass, carbon, kelvar etc. These two constituents, polymer and fibers are mixed at macro level to achieve the properties not attainable by any of them individually. High specific stiffness, high specific strength coupled with controlled anisotropy and superior fatigue strength make the composite materials suitable for many applications.

Lamina or ply is a single layer of unwoven unidirectional reinforcement or woven multidirectional. As this single lamina is generally too thin to be used in any engineering application, several laminae are bonded together to form a thick structure known as 'laminate'.

Laminated composite material found their application in many fields which includes aerospace industry (spaceship, military aircraft), transportation (automobile, boats), electronics industry (Printed Circuit Boards, i.e. PCBs), sports (tennis rackets), helmets etc.

1.2 FAILURE OF COMPOSITES

In an engineering application, when materials start performing unsatisfactorily, it is considered to be failed. The unsatisfactory performance may be due to the limit of stiffness, plastic deformation or complete fracture. In case of composite materials, internal material failure generally initiates much before any change in its macroscopic appearance. The failure of polymer composite can be broadly classified as,

(1) breaking of fibers
(2) microbuckling of fibers
(3) separation of fibers from the matrix known as debonding
(4) separation of laminae from each other in laminated composites known as delamination.

All the above causes initiate the failure, which leads to complete damage of composite structure. Among the mentioned causes, delamination predominates over others. The resistance to crack propagation by delamination is characterised by fracture toughness i.e. energy dissipation on creation of new surfaces. Interlaminar Fracture Toughness of fiber reinforced composites depends on several factors, for example, toughness of matrix, fiber volume fraction, bonding between matrix and fiber, ply angle etc.

Delamination in composites may initiate during manufacturing process due to non-optimum curing or introduction of foreign bodies. This may also result from impact damage, three-dimensional stresses at free edges or discontinuities in the material. The impact of an object on composite laminate causes intense damage at center of impact and induces delamination between the layers of laminate which propagate laterally as delamination cracks.

1.3 LITERATURE SURVEY

In the early attempt by Rybicki et al.(1997) to predict delamination behaviour of laminates, it was realised that critical strain energy release rate may be an useful criterion for study of delamination growth. They modeled the edge delamination as an interface crack at the free edges and analysed it on the basis of fracture mechanics (strain energy release rate).

The concept of delamination prediction on the basis of strain energy release rate was further explored by many investigators. Most of them used Double Cantilever Beam(DCB) specimen to determine critical strain energy release rate in mode I (G_{Ic}) (Devitt et al., 1980, Wang et al., 1995 etc.). Large displacement and small strain theory was used to obtain Interlaminar Fracture Toughness (IFT) as a function of crack propagation with DCB specimen by Devitt et al., 1980.

Bezhenov (1991) conducted experiments on DCB specimen of woven-fabric reinforced laminates to find out G_{Ic}. In his conclusion, he claimed, at very large bending of cantilevers (bend angle greater than 72^0) the critical crack extension force does not depend on crack length. Also the IFT of fabric reinforced laminates is significantly higher than IFT of non-woven unidirectional composites and crack propagation between the layers in both cases is unstable. In an ordinary bending, G_{Ic} values increases as crack grows in length (Lee S.M.,1992).

The influence of stacking sequence on laminar strength is recognized in the beginning itself (Pagano et al., 1971). Wang (1983) used fracture mechanics approach to well known delamination problem and found that fiber orientation, ply thickness and stacking sequence influence the delamination crack behaviour significantly. Kumar (1993) later on suggested a special laminate having stacking sequence $[0/\theta/\theta/0/\theta/0/0/\theta\,|\,0/\theta/\theta/0/\theta/0/0/\theta]$. This laminate minimises bending components D16, D26 in addition to nullify the coupling stiffness matrix [B].

Alberston et al., 1995 studied delamination growth in laminated composites in three stages namely, initiation, slow growth and ply separation. The

initiation fracture toughness of cast precrack of specimen is always greater than the propagation fracture toughness. This may happen due to a resin rich pocket formed ahead of the precrack, which can lead to erroneous high initiation value of G_c. So extending the crack beyond this resin rich pocket is necessary to avoid very high result. The initiation fracture toughness is influenced by fiber/matrix bond strength and matrix ductility, whereas, the propagation toughness is influenced by fiber bridging in addition to above factors.

Kearly et al. (1985) evaluated and compared mode I interlaminar fracture toughness using three different approaches namely J-integral, compliance calibration and analytical equation based on linear bending with DCB specimen. They were at conclusion that Interlaminar Fracture Toughness was over estimated by later two approaches.

Sarkar et al. (1991) dealt with mode I Interlaminar Fracture Toughness of multidirectional laminated composites whose fracture is dominated by matrix fracture. They used both stress approach and energy approach and concluded that energy approach is more accurate than stress approach.

Though most of the investigators used straight DCB specimen in their research, some other investigators used Width Tapered DCB (WTDCB) specimen to calculate interlaminar fracture toughness in mode I (e.g. Bascom et al., 1980, Kyung et al., 1981). The interlaminar fracture behaviour of glass and graphite fabric composite was studied by Bascom et al. (1980) using WTDCB specimen. The compliance and fracture behaviour of specimen as well as effect of specimen geometry on fracture energy using WTDCB specimen were studied for a glass fiber reinforced polyester composites by Kyung et al. (1981). Later it has been realised that G_{Ic} is not affected by width, whereas G_{IIc} is width dependent (Davies et al., 1990).

The loading rate effect on both initiation and propagation of delamination growth under mode I loading condition was studied, using DCB specimen, by many investigators (Miller et al., 1981, Mall et al., 1987, Khalil, 1991 etc.)

Another method for determining the critical strain energy release rate was proposed by Doxee et al. (1993). It was suggested that G_{Ic} can be determined fitting a curve for data of delamination energy vs. delamination area. In this study, carbon/epoxy square specimens with a sequence of $[0_4/90_4]$ and with circular precrack were used.

In a recent study, Kumar & Reddy (1997) have developed a new technique to determine G_{Ic} in plexiglass specimen with a circular fully embedded center crack. This method was named Embedded Crack Plate (ECP) test method. The idea behind this method is that it closely resembles with many practical problems. The method consists of subjecting a circular bonded plate specimen made of plexiglass with fully embedded circular crack to mode I loading. The circular crack front was observed to grow concentrically. The G_{Ic} was found lower than that of DCB specimen.

These days finite element method (FEM) has become a popular technique for the estimation of strain energy release rate G in fracture mechanics. Irvin (1957) introduced the concept of crack closure integral technique. The strain energy release rate can be estimated by the crack closure integral concept by considering an incremental crack extension and evaluating the work done to close the crack to the original configuration. Finite Element formulation equivalent to above concept is done and used to calculate the strain energy release rate, known as Virtual Crack Closure Integral (VCCI) technique.

Rybicki et al., 1977, has proposed a finite element technique to calculate the strain energy release rate based on concept of crack closure integral. The proposed method involves only one analysis as compared to two analyses required in original crack closure integral technique. They called the method as 'Modified Crack Closure Integral (MCCI)' technique.

Falzon et al., 1999, has formulated 3D composite element and used it in a mixed mode fracture mechanics. This element like a conventional 3D element, has three degree of freedom per node. Although like a plate element, strains are defined in local directions of mid-plane surface. The stress-strain property matrix was modified to prevent the element from being too stiff in bending. A main

advantage of this formulation is the ability to model a laminate with a single 3D element so that computational efficiency is enhanced for calculation of strain energy release rates in laminated composites.

B. Raj Kumar, 1998, has done some preliminary experiments on Embedded Crack Plate (ECP) specimen made of unidirectional GFRP laminate and analysed the experimental data on NISA package. His results reveal that the IFT in mid plane is nearly ten times higher in 90° direction compared to 0° direction for laminates $[0°/90°]_{8S}$ and $[0°/45°/-45°/90°/90°/-45°/45°/0°]_S$.

1.4 OUTLINE OF THE PRESENT WORK

An experimental-numerical technique is developed to determine Interlaminar Fracture Toughness of FRP composites through an Embedded Crack Plate (ECP) specimen. This method is an extension of the technique developed by Kumar & Reddy (1997) on a specimen made of isotropic material e.g. plexiglass. Experiments are conducted on FRP plates with an embedded crack to determine critical loads and corresponding crack fronts of interlaminar crack. A numerical technique is developed and applied to ECP specimen of FRP composites to determine its G_{Ic}.

1.5 ORGANISATION OF THE THESIS

Chapter 1 deals with the introduction and briefing about some of the work done in the field of determining fracture toughness of composites. In Ch.2, the concept of energy release rate is introduced and some important experimental techniques and finite element technique to determine energy release rate are discussed. In Ch.3, the experimental numerical technique is validated by comparing its results with analytical results. In Ch.4, the experimental-numerical technique is applied to FRP composite laminates and the results and discussions are dealt with. The entire work is then concluded in Ch.5 along with suggestions for future work.

CHAPTER-2
ENERGY RELEASE RATE

2.1 INTRODUCTION

Advanced fiber reinforced composite materials have been in use for over four decades. The biggest drawback, which has been noticed, is its low resistance to delamination. Delamination in laminates not only leads to complete fracture but also decreases its stiffness, which is very important design consideration for designers. In the present scenario, it is the challenge among the researchers to reduce the delaminating behaviour of composites in order to increase its life and load bearing capability of composite structures.

The measurement of delamination toughness of composites is quite important for the comparative study. The parameter Energy Release Rate suits for studying delamination cracks in composites because the crack plane is well defined and material remains elastic in the vicinity of the crack tip except in the very thin layer of the interface.

In this chapter, we introduce with the concept of Energy Release Rate and different ways to determine its value analytically and then through Finite Element Method for Double Cantilever Beam (DCB) and Embedded Crack Plate (ECP) specimens.

2.2 ENERGY RELEASE RATE

There are two important parameters involved in any crack growing process. One is the Energy Release Rate and other is Crack Resistance. There is always an energy release from the body when a crack moves and at the same time energy required for the formation of new surfaces. The energy release is measured by the parameter, Energy Release Rate, G. The Energy Release rate is defined as energy release per unit area extension of crack growth. Also the energy required to form new crack surfaces is accounted by the parameter, Crack Resistance, R. The Crack Resistance is defined as the energy required for a crack to grow by unit area.

Mathematical formulation for energy release rate is carried out by invoking the conservation of energy. Consider a body having a crack of length 'a'. If the crack grows by Δa then the incremental increase in the crack area is ΔA. For an incremental external work, ΔW_{ext}, by the external forces, strain energy balance is given by,

$$G \cdot \Delta A = \Delta W_{ext} - \Delta U \tag{2.1}$$

where 'A' is the area of the crack. Dividing the equation by ΔA and taking the limit $\Delta A \rightarrow 0$, we obtain,

$$G = -\frac{d(U - W_{ext})}{dA}. \tag{2.2}$$

But $(U - W_{ext})$ is commonly known as potential energy Π. Therefore, the above equation is written as

$$G = -\frac{d\Pi}{dA}. \tag{2.3}$$

Now consider general case of a body with a crack and load P acting as shown in Fig 2.1. The displacement, u of the points at which load is applied can be written as,

$$u = C \cdot P \tag{2.4}$$

where C is compliance.

Strain energy is then expressed as,

$$U=\frac{1}{2}Pu$$

$$=\frac{1}{2}C.P^2.$$

Differentiating, one obtains,

$$dU=CPdP+\frac{P^2}{2}dC. \tag{2.5}$$

External Work done is given by,

$$dW_{ext}=Pdu.$$

Differentiating Eq.2.4 and substituting, one obtains,

$$dW_{ext}=PCdP+P^2dC \tag{2.6}$$

Substituting from Eq. 2.4 & 2.5 into Eq. 2.2, we get,

$$G=\frac{P^2}{2}.\frac{dC}{dA}. \tag{2.7}$$

For a special case of DCB specimen of thickness 'b', dA=b.da and then

$$G=\frac{P^2}{2b}\frac{dC}{da}. \tag{2.8}$$

When a body with a crack is loaded, the crack propagation begins at a specified load. Depending on the initial crack length, the crack may be stable or unstable. The necessary conditions for the crack advance are

- $G \geq R$ (2.9)
- $dG/da \geq dR/da$ (2.10)

The value of G which satisfies these two conditions become material property and is known as Critical Energy Release Rate, G_c.

2.3 METHODS TO DETERMINE G_{Ic}

There are two approaches to determine Fracture Toughness (G_{Ic}). One is based on experimental and analytical procedure and other is based on experimental and numerical procedure.

2.3.1 Experimental-Analytical Methods

In determining the Critical Energy Release Rate(G_{Ic}) or fracture toughness of any material, the test methods used play very important role. There are several test methods to determine the Energy Release Rate.

- Area method with DCB specimen
- Compliance method with DCB specimen
- Angle method with DCB specimen
- Embedded Crack Plate(ECP) test method

Area Method with DCB Specimen

This is the easiest method to understand and to analyse. This method utilises the area under load displacement diagram obtained from an experiment to calculate the Energy Release Rate, G. To describe the method, a DCB specimen is used whose geometry is shown in Fig 2.2. This specimen with initial crack length a_0 is loaded in 'displacement controlled mode' in a tensile testing machine. After certain load, the crack starts growing. As soon as crack grows by a small distance machine is stopped and the crack is allowed to grow until it arrests by itself. Then the specimen is unloaded to zero load. Now consider the shaded area O-A-B-O in the Fig 2.3. The energy released on propagation of a crack from point A to point B is equal to the area of triangle-like figure O-A-B. Considering the area of triangle 'OAB', the Energy Release Rate can be expressed as (Kumar, 1999);

$$G_{Ic} = \frac{\text{Area of } \Delta OAB}{b.\Delta a} \qquad (2.11)$$

Though the area method is very simple for rough estimation of Energy Release Rate, it is tedious to calculate area to find G_{Ic}. Other drawback with this method is that data processing does not minimise the effect of local factors such as non-uniform bonding, fibre concentration etc.

Compliance Method with DCB Specimen

The compliance method using Double Cantilever Beam (DCB) specimen has been widely used for measurement of interlaminar fracture toughness in mode I. The deflection of cantilever beam, δ, caused by load P applied at the free end is given as,

$$\delta = \frac{PL^3}{3EI} \tag{2.12}$$

where, L = length of cantilever arm,

E = modulus of elasticity of material, and

I = moment of inertia of beam cross section.

For DCB specimen under a load as shown in Fig 2.2, the cracked portion behaves as two independent cantilevers of length 'a'. Therefore, the relative displacement of the load points is

$$u = 2 \cdot \frac{Pa^3}{3EI} \tag{2.13}$$

and the compliance C is given by,

$$C = \frac{u}{P} = \frac{2a^3}{3EI}. \tag{2.14}$$

Differentiating the equation with respect to 'a' and substituting in Eq.(2.8) we arrive at

$$G_I = \frac{1}{b} \cdot \frac{P^2 a^2}{EI}. \tag{2.15}$$

If we use above equation directly, it requires material property E and geometric property I, to be evaluated from separate tests. But it is possible to calculate G_I without determining E & I through separate tests and measurements.

Eq.(2.14) can be written as

$$C = A_1 \cdot a^3 \tag{2.16}$$

Where,

$$A_1 = \frac{2}{3EI}. \tag{2.17}$$

Similarly, Eq.(2.15) can also be written as

$$P = \frac{\sqrt{G_I EIb}}{a} = \frac{A_2}{a} \tag{2.18}$$

where

$$A_2 = \sqrt{G_I EIb} \tag{2.19}$$

By eliminating flexural rigidity, EI from Eqs. (2.17) & (2.18), we obtain,

$$G_I = \frac{3}{2}\frac{A_1 A_2^{\,2}}{b}. \tag{2.20}$$

The G_I becomes material property G_{Ic}, when load applied is critical load. Therefore, G_{Ic} can be evaluated by knowing A_1 & A_2. It is worth noting that A_1 & A_2 are constants for a given specimen and can be evaluated from experimental data obtained from DCB test and using an approximate data reduction technique (Kumar, 1999) discussed in Appendix-A. This is a laborious technique, as it requires compliance to be evaluated for several values of crack length to evaluate A_1 & A_2.

Angle Method with DCB Specimen

Recently a new method is reported to calculate Interlaminar Fracture Toughness G_{Ic}, through a DCB specimen by Bezhenov (1995). In this method the same test procedure as used above is used along with an additional input of set of photographs taken periodically to calculate the angles of the cantilever beams, α_1 and α_2. In this method, elastic-bending theory is used to derive G_{Ic}. The DCB specimen is fixed at an angle α_C and the load is applied vertically at the left end of the beam as shown in Fig 2.4.

According to the elastic theory, the fracture toughness at the fixed load or fixed jaw for DCB specimen is given by,

$$G_{Ic} = -\frac{1}{b}\frac{\partial U}{\partial a} \tag{2.21}$$

The strain energy U of a beam is given by

$$U = \int_0^a \frac{M^2}{2EI} da \qquad (2.22)$$

where

M= bending moment

E = effective young's modulus

I = second moment of inertia of cross section about the bending axis

A = crack length

Substituting the Eq.(2.22) in Eq.(2.21) and considering both cantilever arms, the following equation can be obtained

$$G_{Ic} = \frac{M_C^2}{2b(EI)_1} + \frac{M_C^2}{2b(EI)_2} = \frac{M_C^2}{2b}\left(\frac{1}{(EI)_1} + \frac{1}{(EI)_2}\right) \qquad (2.23)$$

Where, M_C = critical bending moment

If the bending is symmetrical i.e. $\alpha_C = 0$, the above Eq. Can be reduced to-

$$G_{IC} = \frac{P_C}{b}(\sin\alpha_1 + \sin\alpha_2) \qquad (2.24)$$

Where

P_C = crack propagation force

α_1 = Bend angle of first cantilever arm at load point

α_2 = Bend angle of second cantilever arm at load point

b= width of the beam

Angles α_1 and α_2 are measured from the photographs taken during the DCB test using a low magnification optical microscope that allows an accurate determination of angles. This method may be used with weak, intermediate or highly stiff DCB specimens. This method necessitates use of a camera during testing and subsequent development of films and measurement of angles on the photographs, which is time-consuming process.

Embedded crack plate (ECP) test method

A new test method to determine the Energy Release Rate is developed by Kumar & Reddy, 1997. This method deals with the determination of Interlaminar Fracture Toughness of materials strictly in mode I loading. In this method, a penny shaped (circular) crack is embedded between two layers of isotropic materials. Its mathematical formulation to determine G_I is presented below.

Consider two circular plates, each of thickness t, bonded together with an embedded penny precrack of radius 'a'. When the load is applied at the centre as shown in the Fig 2.5, the crack will grow in the crack plane. The problem can be modelled with a single plate of thickness t and radius of 'a', with fixed boundary conditions at the edge and load applied in centre at periphery of the circle of radius r_0. When $r_0 << a$, deflection at centre is deduced (From "Roark's Formulas for Stress and Strain", W.C. Young, 1989) as

$$\delta = \frac{3}{4}\frac{Pa^2(1-\upsilon^2)}{\pi Et^3} \tag{2.25}$$

where 't' is the thickness of the plate, E is the Young's modulus and υ is the Poisson's ratio. The above equation can be expressed as,

$$\delta = \frac{Pa^2}{16\pi\eta} \tag{2.26}$$

where flexural rigidity η is defined as,

$$\eta = \frac{Et^3}{12(1-\upsilon^2)}. \tag{2.27}$$

When the thickness and the flexural rigidity of top and bottom plates are same then the relative displacement of the load points is given by

$$u = \frac{Pa^2}{8\pi\eta} \tag{2.28}$$

$$= \frac{P\pi a^2}{8\pi^2\eta} = \frac{P.A}{8\pi^2\eta}$$

where 'A' is the area of cracked portion.

The compliance is given by,

$$C = \frac{u}{P} = \frac{A}{8\pi^2\eta}. \tag{2.29}$$

Substituting the Compliance 'C' in Eq (2.7)

$$G_I = \frac{P^2}{16\pi^2\eta}. \tag{2.30}$$

Substituting η from the Eq (2.25) we have,

$$G_I = \frac{3P^2}{4\pi^2}\frac{(1-\nu^2)}{Et^3}. \tag{2.31}$$

From the above equation it is clear that Energy Release Rate in ECP test is independent of size of crack length 'a' whereas G_I in DCB test is proportional to square of the crack length. Also in ECP test, crack growth is metastable under load control mode in contrast to unstable growth in DCB test. In the displacement control mode crack growth is stable and the load required to propagate the crack is expected not to change with radius of the penny crack.

2.3.2 EXPERIMENTAL-NUMERICAL METHOD

The fracture mechanics principals coupled with finite element analysis is used to predict failure in composite structures, which has received much attention in recent years. There are two numerical methods discussed below to determine the Energy Release Rate.

Virtual Crack Closure Integral (VCCI) Technique

Irwin proposed this method in 1957. It was originally an integral formulation, which requires finite element solution for numerical analysis to predict the Energy Release Rate resulting from the growth of crack by a predetermined length.

The Virtual Crack Closure Integral technique is based on the assumption that the energy required to propagate a crack by a small amount ' Δa ' is equal to the work required to close the crack by the same amount.

For a 2D crack configuration with mode I loading in DCB specimen

$$G_I = \lim_{\Delta a \to 0}\left\{\frac{1}{2\Delta a}\int_0^{\Delta a}\sigma_{ZZ}(x,0)\cdot\omega(x-\Delta a,0)dx\right\} \tag{2.32}$$

where ω is the displacement in Z-direction(normal to the specimen surface).

The corresponding finite element formulation is

$$G_I = \lim_{\Delta a \to 0}\frac{1}{2\Delta a.b}\left[\{F_{ZZ}^T\}\{\omega\}\right]. \tag{2.33}$$

where F is nodal force vector required to close the crack by an amount Δa and ω is displacement vector of respective nodes when there is no crack closure force vector F.

This may be extended to embedded crack in a plate with the crack front in the 'y' direction as

$$G_I = \lim_{\Delta a \to 0}\left\{\frac{1}{2\Delta a\cdot\Delta y}\int_y^{y+\Delta y}\left[\int_0^{\Delta a}\sigma_{ZZ}(x,y,0)\cdot\omega(x-\Delta a,y,0)dx\right]dy\right\} \tag{2.34}$$

Procedures involved in calculating the G_I value are shown in Figs. 2.6-2.8. In the case of 2D, we determine constraint force at the node on the crack tip and then the displacement of the same node when crack moves by very small amount, say Δa (i.e. releasing the node at the crack front), as shown in Fig 2.6. Considering the gradual growth of crack one obtains,

$$G_I = \frac{1}{2\Delta a.b}(F_Z\cdot\delta_Z) \tag{2.35}$$

For the case of higher order elements like 8-noded 2D elements as in Fig 2.7, procedures adopted are same as 4-noded 2D elements. In case (a), we determine the constraint force F_{Z1} at the node on crack front '1'. Now move the crack front to '2' as shown in case (b) and determine δ_{Z1} (i.e. displacement of node at previous crack-front) and F_{Z2} (i.e. constraint force at node at new crack front 2).

Now again move the crack-front to '3' and then determine δ_{Z2} (i.e. displacement of node at previous crack-front '2').

Now,

$$G_I = \frac{\frac{1}{2}F_{Z1}\delta_{Z1} + \frac{1}{2}F_{Z2}\delta_{Z2}}{b.\Delta a} \tag{2.36}$$

The same method is adopted for 8-noded 3D brick elements and 20-noded 3D brick elements.

For 3D 20-noded brick elements as shown in Fig. 2.8,

$$G_I = \frac{\frac{1}{2}F_{Z1}\left(\omega_1 - \omega_{1'}\right) + \frac{1}{2}F_{Z2}\left(\omega_2 - \omega_{2'}\right) + \frac{1}{2}F_{Z3}\left(\omega_3 - \omega_{3'}\right) + \frac{1}{2}F_{Z4}\left(\omega_4 - \omega_{4'}\right) + \frac{1}{2}F_{Z5}\left(\omega_5 - \omega_{5'}\right)}{\Delta y \Delta a} \tag{2.37}$$

FE analysis using VCCI technique requires two passes and for higher order elements requires three passes. For higher order elements, first pass is to find holding force of end nodes, second pass to find unrestrained displacement of end nodes and holding force of mid nodes and third pass to find unrestrained displacement of mid nodes. Thus, VCCI technique for higher order is computationally expensive.

Modified Crack Closure Integral (MCCI) Technique.

The above VCCI technique being computationally expensive was being modified by Rybicki (E.F.Rybicki et.al., 1977) and known as Modified Crack Closure Integral (MCCI) technique. In this method Energy Release Rate, G_I is calculated at the crack tip by using forces at the crack tip and displacements behind the crack tip for very small crack extension ($\Delta a << a$).

For 2D 4-noded isoparametric elements in Fig.2.6(b),

$$G_I = \frac{\frac{1}{2}F_{Z2}\left(\omega_1 - \omega_{1'}\right)}{b.\Delta a} \tag{2.38}$$

For 2D 8-noded isoparametric elements in Fig.2.7(c),

$$G_1 = \frac{\frac{1}{2}F_{Z3}(\omega_1 - \omega_{1'}) + \frac{1}{2}F_{Z4}(\omega_2 - \omega_{2'})}{b.\Delta a} \qquad (2.39)$$

For 3D 20-noded brick elements (Fig.2.8),

$$G_1 = \frac{\frac{1}{2}F_{Z6}(\omega_1 - \omega_{1'}) + \frac{1}{2}F_{Z8}(\omega_2 - \omega_{2'}) + \frac{1}{2}F_{Z7}(\omega_3 - \omega_{3'}) + \frac{1}{2}F_{Z9}(\omega_4 - \omega_{4'}) + \frac{1}{2}F_{Z10}(\omega_5 - \omega_{5'})}{\Delta y \Delta a} \qquad (2.40)$$

The MCCI technique requires only single pass to calculate G_I, so it is computationally efficient. But it is relatively less accurate than VCCI technique. Accuracy can be enhanced by using very fine mesh near the crack tip. In the present study MCCI technique is adopted for DCB specimens and VCCI technique is adopted for Embedded Crack Plate(ECP) specimen because in ECP specimen width of the crack front increases as the crack grows radially but in DCB specimen, width of the crack front remains constant.

2.4 CLOSURE

DCB test has gained wide popularity in last two and half decades to calculate Interlaminar Energy Release Rate. The Compliance Method is widely accepted out of available DCB test methods. However, it is laborious technique to determine compliance for several crack lengths. A method called Angle Method has been developed recently and claims that it can be used for high and low stiff beams.

A new method has been developed and formulated by Kumar & Reddy, 1997, to determine Interlaminar Energy Release Rate by using circular specimen in which a circular precrack is embedded. The method is known as Embedded Crack Plate (ECP) test method. In ECP test method, crack front obtained through experiments is nearly circular; so close form results developed can be used to determine the Energy Release Rate. This method is quite reasonable for strictly mode I loading with no end effects.

These days, numerical methods like VCCI, & MCCI techniques are developed to determine Energy Release Rate. In the next chapter these methods are tested for DCB & ECP specimens on isotropic materials for which close form solutions are available. Once we get the satisfying results, these methods will be used for anisotropic materials in chapter-4.

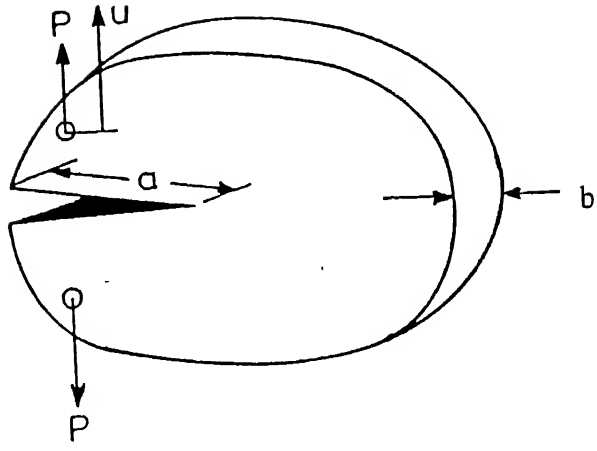

Fig.2.1 A plate with a crack.

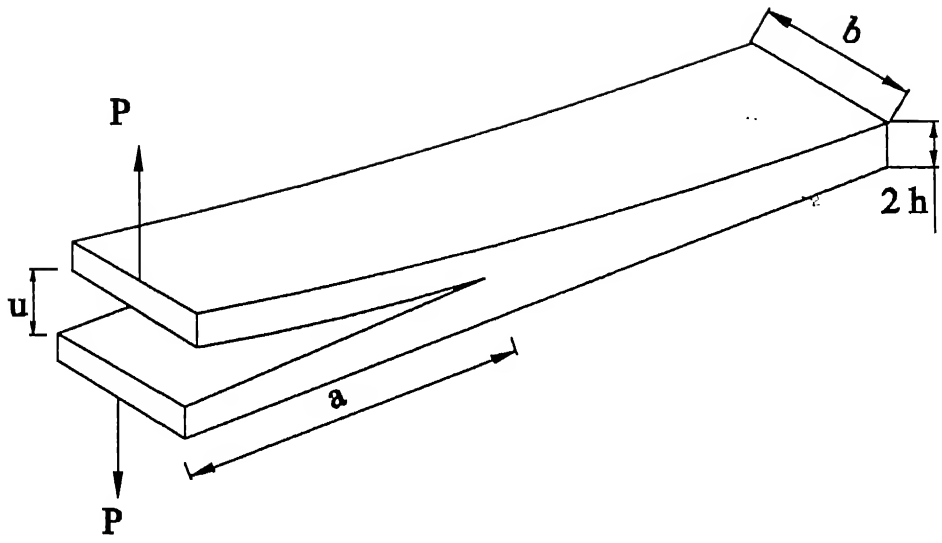

Fig. 2.2 DCB Specimen loaded in mode I.

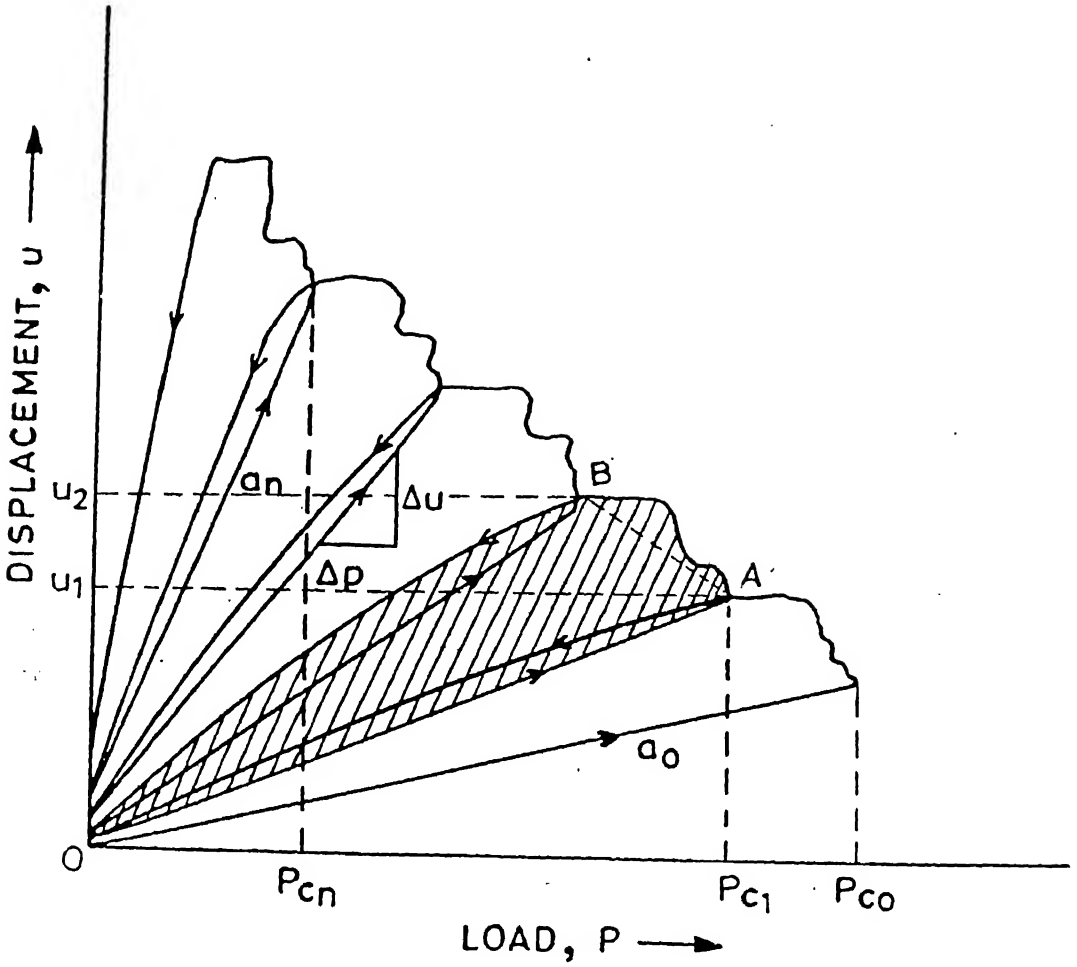

Fig.2.3 An illustration of Area method.

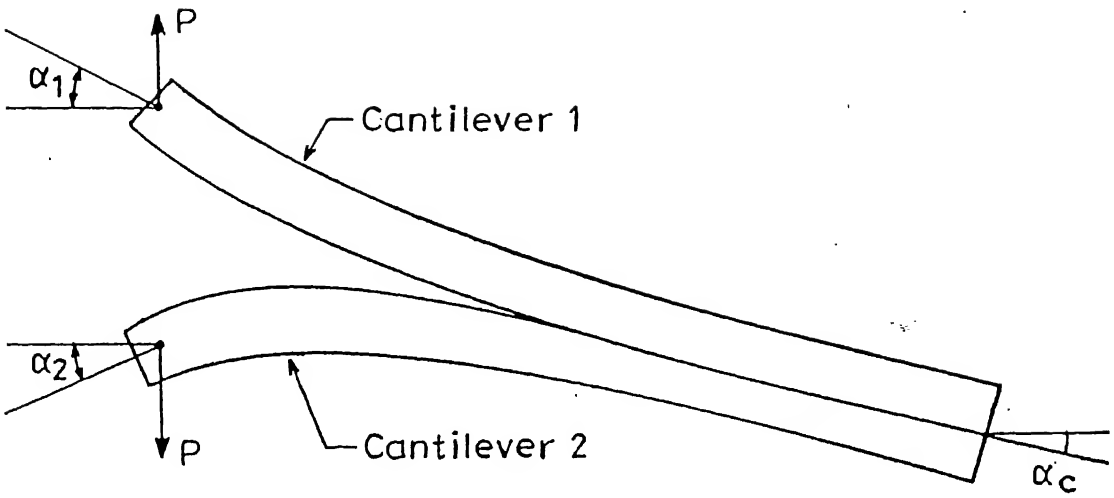

Fig.2.4 Illustration of Angle method by DCB specimen.

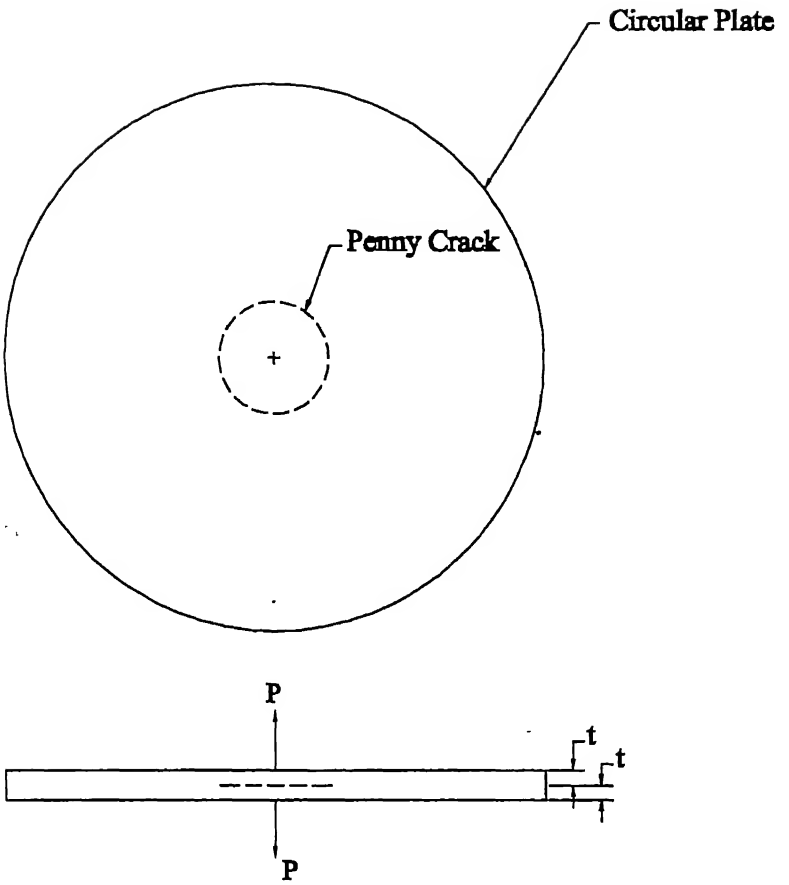

Fig. 2.5 A typical ECP specimen

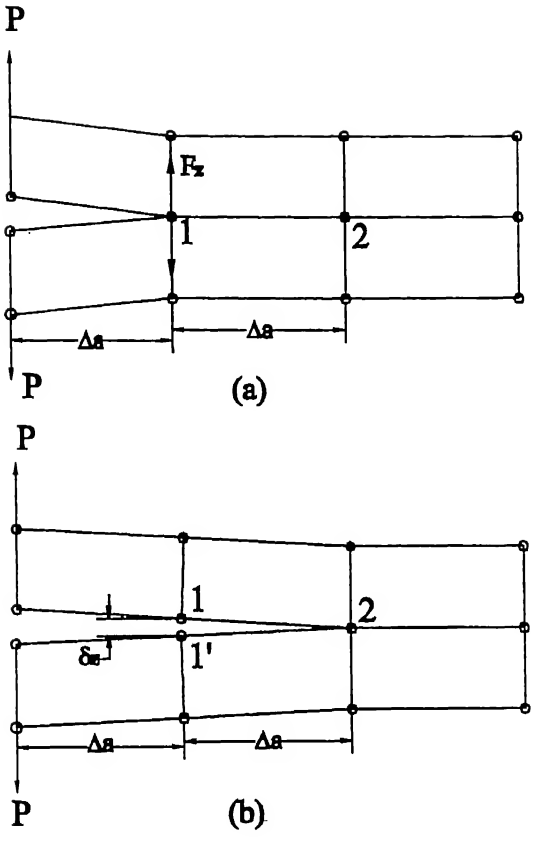

Fig. 2.6 An illustration for Crack growth using 2D 4-noded elements

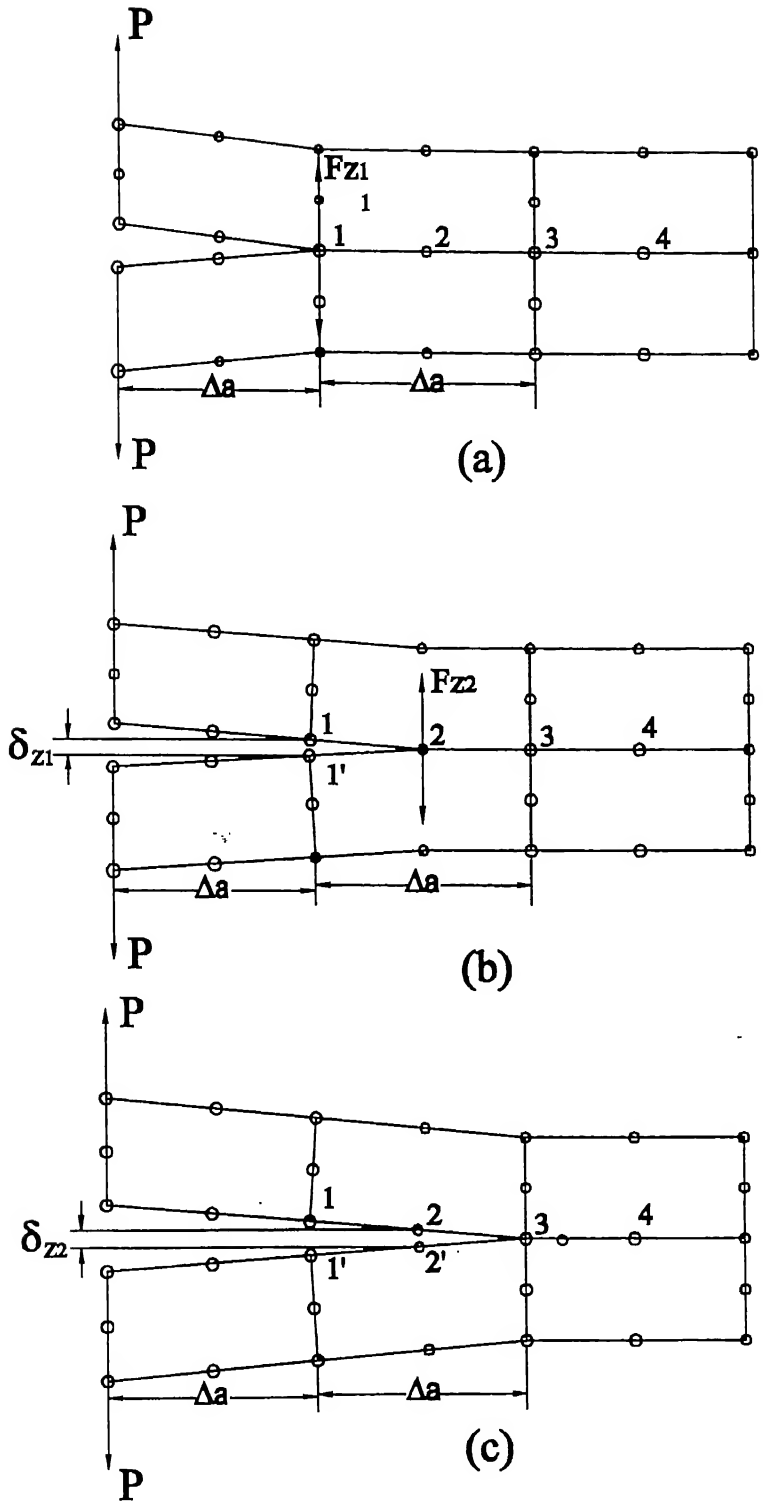

Fig. 2.7 An illustration of Crack growth in 2D using 8-noded elements

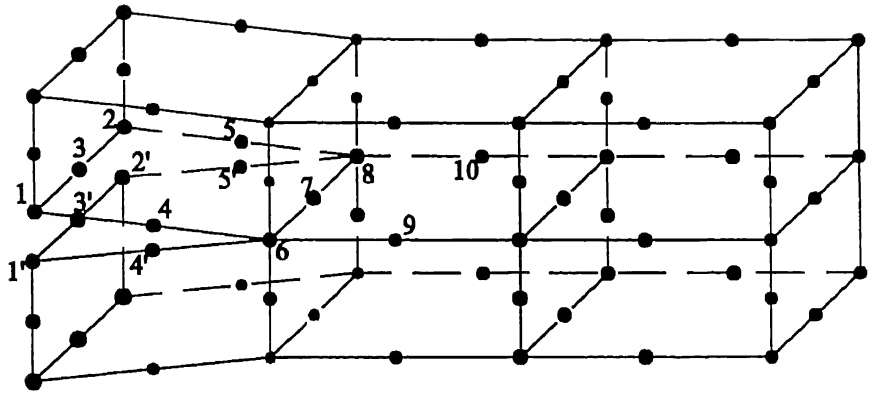

Fig.2.8 An Illustration for Embedded Crack Growth in 3D Using 20-Noded Brick Elements

CHAPTER-3

VALIDATION OF NUMERICAL TECHNIQUE

3.1 INTRODUCTION

To determine a material property, it is desirable to develop a technique for which data analysis is available through closed form theoretical formulation. However with increasing sophistication, a rigorous model may not be available and in certain cases of practical interest, a closed form analysis may not be available. Under such conditions one may resort to numerical analysis and develop techniques to determine toughness through Experimental-Numerical technique. In fact, one should no longer be afraid of numerical analysis because powerful computers are available at very reasonable prices and enough know-how has been generated to develop user friendly packages.

In the present study, finite element analysis is developed for DCB & ECP specimens of isotropic materials and their validity are checked by comparing deflection and fracture toughness in mode I (G_{Ic}), determined through analytical methods.

In this chapter, Virtual Crack Closure Integral (VCCI) technique is used for ECP specimens & Modified Crack Closure Integral (MCCI) technique for DCB specimen to determine Interlaminar Fracture Toughness in mode I (G_{Ic}) through numerical method and their results are compared by analytical methods. The analytical method for DCB specimen is well known, by finding compliance (Eq.2.15) and for ECP specimens, the analytical method as developed by Kumar & Reddy (1997), is presented in Sec.2.

Once the numerical method is proved on isotropic specimen, it can be used for more complex problems like laminated composite materials for which analytical methods may not be available in a few cases.

3.2 FINITE ELEMENT METHOD IN 3D SOLID MECHANICS

Finite element method is a powerful technique for approximate solution of continuum mechanics. It is an approximate method, because a continuum with infinite number of degrees of freedom is replaced with a discrete system with finite number of degrees of freedom. The method involves subdividing the continuum in to a finite number of regions called elements connected at finite number of points called node. An approximate solution is constructed over the assemblage of elements and solution continuity is maintained at inter-element boundary.

Solid mechanics deals with the general formulation and solution of deformable bodies subjected to forces and displacements. Any body subjected to external forces (body forces, surface forces) is, in general, described by the following variables equations.

(1) VARIABLES:

Displacements: u, v, w which are functions of (x, y, z)

Strain components: ϵ_x, ϵ_y, ϵ_z, γ_{xy}, γ_{yz}, γ_{zx}

Stress components: σ_x, σ_y, σ_z, σ_{xy}, σ_{yz}, σ_{zx}

(2) RELATIONSHIP BETWEEN VARIABLES:

Strain-displacement relations:

$$\epsilon_x = \frac{\partial u}{\partial x},\ \epsilon_y = \frac{\partial v}{\partial y},\ \epsilon_z = \frac{\partial w}{\partial z}$$

$$\gamma_{xy} = \frac{\partial u}{\partial y} + \frac{\partial v}{\partial x},\ \gamma_{yz} = \frac{\partial v}{\partial z} + \frac{\partial w}{\partial y},\ \gamma_{zx} = \frac{\partial w}{\partial x} + \frac{\partial u}{\partial z}$$

Stress-strain relations for linear elastic 3D orthotropic materials

$$\begin{Bmatrix} \varepsilon_x \\ \varepsilon_y \\ \varepsilon_z \\ \varepsilon_{xy} \\ \varepsilon_{yz} \\ \varepsilon_{xz} \end{Bmatrix} = \begin{bmatrix} \frac{1}{E_x} & \frac{-\nu_{yx}}{E_y} & \frac{-\nu_{zx}}{E_z} & 0 & 0 & 0 \\ \frac{-\nu_{xy}}{E_x} & \frac{1}{E_y} & \frac{-\nu_{zy}}{E_z} & 0 & 0 & 0 \\ \frac{-\nu_{xz}}{E_x} & \frac{-\nu_{yz}}{E_y} & \frac{1}{E_z} & 0 & 0 & 0 \\ 0 & 0 & 0 & \frac{1}{G_{xy}} & 0 & 0 \\ 0 & 0 & 0 & 0 & \frac{1}{G_{yz}} & 0 \\ 0 & 0 & 0 & 0 & 0 & \frac{1}{G_{xz}} \end{bmatrix} \begin{Bmatrix} \sigma_x \\ \sigma_y \\ \sigma_z \\ \sigma_{xy} \\ \sigma_{yz} \\ \sigma_{xz} \end{Bmatrix} \tag{3.1}$$

(3) GOVERNING EQUILIBRIUM EQUATIONS:

$$\frac{\partial \sigma_x}{\partial x} + \frac{\partial \tau_{xy}}{\partial y} + \frac{\partial \tau_{xz}}{\partial z} + \bar{X} = 0$$

$$\frac{\partial \tau_{xy}}{\partial x} + \frac{\partial \sigma_y}{\partial y} + \frac{\partial \tau_{yz}}{\partial z} + \bar{Y} = 0$$

$$\frac{\partial \tau_{xz}}{\partial x} + \frac{\partial \tau_{yz}}{\partial y} + \frac{\partial \sigma_z}{\partial z} + \bar{Z} = 0 \tag{3.2}$$

where $\bar{X}$, $\bar{Y}$, $\bar{Z}$ are body forces along X,Y,Z directions

(4) BOUNDARY CONDITIONS

Prescribed displacements: $u = \bar{u}$, $v = \bar{v}$, $w = \bar{w}$ on Γ_u

Prescribed tractions on Γ_q

$$\sigma_x n_x + \tau_{xy} n_y + \tau_{xz} n_z = \bar{t}_x$$

$$\tau_{xy} n_x + \sigma_y n_y + \tau_{yz} n_z = \bar{t}_y$$

$$\tau_{xz} n_x + \tau_{yz} n_y + \sigma_z n_z = \bar{t}_z \tag{3.3}$$

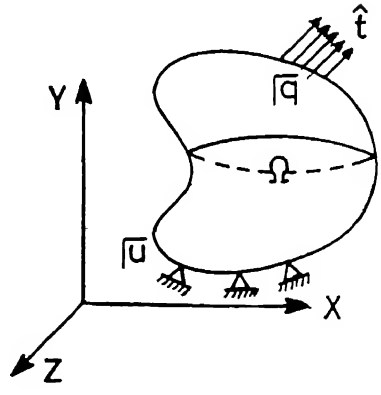

(5) COMPATIBILITY CONDITIONS:

The fundamental aspect of these equations is that the points, which are neighbours in undeformed configuration, do remain neighbours after deformations.

$$\frac{\partial^2 \varepsilon_{xx}}{\partial y^2} + \frac{\partial^2 \varepsilon_{yy}}{\partial x^2} = \frac{\partial^2 \gamma_{xy}}{\partial x.\partial y}$$

$$\frac{\partial^2 \varepsilon_{yy}}{\partial z^2} + \frac{\partial^2 \varepsilon_{zz}}{\partial y^2} = \frac{\partial^2 \gamma_{yz}}{\partial y.\partial z}$$

$$\frac{\partial^2 \varepsilon_{zz}}{\partial x^2} + \frac{\partial^2 \varepsilon_{xx}}{\partial z^2} = \frac{\partial^2 \gamma_{zx}}{\partial z.\partial x}$$

$$\frac{\partial}{\partial z}\left(\frac{\partial \gamma_{yz}}{\partial x} + \frac{\partial \gamma_{zx}}{\partial y} - \frac{\partial \gamma_{xy}}{\partial z}\right) = 2\frac{\partial^2 \varepsilon_{zz}}{\partial x.\partial y}$$

$$\frac{\partial}{\partial x}\left(\frac{\partial \gamma_{zx}}{\partial y} + \frac{\partial \gamma_{xy}}{\partial z} - \frac{\partial \gamma_{yz}}{\partial x} = 2\frac{\partial^2 \varepsilon_{xx}}{\partial y.\partial z}\right)$$

$$\frac{\partial}{\partial y}\left(\frac{\partial \gamma_{xy}}{\partial z} + \frac{\partial \gamma_{yz}}{\partial x} - \frac{\partial \gamma_{zx}}{\partial y}\right) = 2\frac{\partial^2 \varepsilon_{yy}}{\partial z.\partial x}$$

3.2.1 FINITE ELEMENTS FORMULATION

Weighted residual statement in generalised load condition can be written as-

$$\int_\Omega \omega_i \left(\frac{\partial \sigma_x}{\partial x} + \frac{\partial \tau_{xy}}{\partial y} + \frac{\partial \tau_{xz}}{\partial z} + \bar{X}\right) d\Omega + \int_{\Gamma_q} \bar{\omega}_i \left(\sigma_x n_x + \tau_{xy} n_y + \tau_{xz} n_z - \bar{t}_x\right) d\Gamma = 0$$

$$\int_\Omega \omega_i \left(\frac{\partial \tau_{xy}}{\partial x} + \frac{\partial \sigma_y}{\partial y} + \frac{\partial \tau_{yz}}{\partial z} + \bar{Y}\right) d\Omega + \int_{\Gamma_q} \bar{\omega}_i \left(\tau_{xy} n_x + \sigma_y n_y + \tau_{yz} n_z - \bar{t}_y\right) d\Gamma = 0$$

$$\int_\Omega \omega_i \left(\frac{\partial \tau_{xz}}{\partial x} + \frac{\partial \tau_{yz}}{\partial y} + \frac{\partial \sigma_z}{\partial z} + \bar{Z}\right) d\Omega + \int_{\Gamma_q} \bar{\omega}_i \left(\tau_{xz} n_x + \tau_{yz} n_y + \sigma_z n_z - \bar{t}_z\right) d\Gamma = 0 \qquad (3.4)$$

Simplifying the above equations and using the relations;

$$\{\sigma\} = [D][B]\{\bar{u}\}$$

where [D] is matrix of material properties, [B] is a matrix for appropriate relation between strain and nodal displacements, one can arrive at (by using the Galerkin Approach),

$$[K]\{u\} = \{f\} \tag{3.5}$$

where $[K] = \sum_e [K_e]$

and, $[K_e] = \int_{\Omega^e} [B]^T [D][B] d\Omega$

$$\{f\} = \sum_e \{f_e\}$$

$$\{f_e\} = \int_e [N_i] \begin{Bmatrix} \bar{X} \\ \bar{Y} \\ \bar{Z} \end{Bmatrix} d\Omega + \int_{\Gamma_q} [N_i] \begin{Bmatrix} \bar{t}_x \\ \bar{t}_y \\ \bar{t}_z \end{Bmatrix} d\Gamma$$

where N_i is shape function.

3.2.2 ELEMENT TYPE:

A 3D 20-noded brick element (also called quadratic hexahedral) is used in the present analysis. The 3D element used is based on general state of stress characterised by six components ($\sigma_x, \sigma_y, \sigma_z, \tau_{xy}, \tau_{yz}, \tau_{xz}$). The element has three translational (u_x, u_y, u_z) and three rotational (θ_x, θ_y, θ_z) degrees of freedom per node. The elements are isoparametric i.e. it has same shape functions for both geometry and dependent variables.

A 20-noded brick element is used for the following reasons.

- The brick elements are suitable for modelling 3D solid structure with general loading.
- Brick elements are able to consider three-dimensional state of stress, which is required in our present study to consider transverse shear deformation.
- A 20-noded element when compared to 8-noded element behaves well in bending due to higher order terms in its formulation

3.3 CALCULATION OF ENERGY RELEASE RATE

Concept to calculate of the Energy Release Rate by numerical method is developed in Ch.2. The method is applied on a DCB & ECP specimens for which analytical results are available. To calculate the G_I value, MCCI technique is applied for DCB specimen and VCCI technique is applied for ECP specimen.

DCB Specimen:

Figure 3.1 shows a DCB specimen loaded in mode I. Due to symmetry in geometry, material property and loading conditions, only half portion (only one cantilever beam) is modelled with the given dimensions on the FEMAP package by using 20-noded brick elements. It is modelled in rectangular co-ordinate system. The boundary conditions are described in Fig.3.2.

For the dimensions of specimen (length l=100mm, width b=30mm, thickness t=2mm), elements in length direction are 56, in width direction 30, and in thickness direction 4. The material used for simulation is mild steel with properties E=207GPa, ν=0.3. Algorithm to determine G_I for DCB specimen by MCCI technique is as follows:

- Create the model with specified boundary conditions and load by 20-noded brick elements on FEMAP.
- Analyse the model by CSA/NASTRAN and import the results.
- Note the holding forces at the nodes on crack front C_2 & curve L_2 (Fig.3.3)and displacements of corresponding nodes on curves C_1 & L_1 lying on the crack plane.
- Multiply the holding forces of nodes in Z-direction (F_z) on C_2 & L_2 with deflection in Z-direction (δ_z) of corresponding nodes on C_1 & L_1 (according to the Eq-2.39), and divide by the area produced by the growth of the crack. This gives the G_I value of DCB specimen.

Eq.2.13 is used to determine closed form results for deflection & Eq-2.15 for Energy Release Rate. The data by analytical analysis and numerical analysis for the specimen are tabulated in Table 3.1 and result is shown in Fig.3.4.

Table 3.1 Deflection and G_I of cantilever for isotropic material

Load (N)	Crack Length a (mm)	Analytical δ (mm)	FEM δ (mm)	Analytical G_I (J/m^2)	FEM G_I (J/m^2)
150	50	3.02	3.1	452.9	450.8

Above results shows that there is good matching of δ and G_I by both analytical and numerical methods for DCB specimen.

ECP Specimen:

Figure 3.5 shows a ECP specimen loaded in mode I. Due to symmetry of geometry, material property and loading, one sixteenth of the specimen is modelled as shown in Fig.3.6 with the specified boundary conditions and load in cylindrical co-ordinate. Material used for simulation is Plexiglass with properties E=3.1GPa, ν=0.33. Due to above symmetry, the specimen can be modelled by a sector with included angle as small as we want with the appropriate load. The boundary conditions are shown in Fig.3.6. Algorithm to find G_I in ECP specimen by VCCI technique (Fig.3.7) is as follows:

(1) Create the model (one sixteenth of the specimen geometry) in cylindrical co-ordinate, apply the load and boundary conditions.

(2) Analyse the model & import the result for analysis.

(3) Find the holding forces of all nodes lying on curve C_1.

(4) Release the nodes on curve C_1, analyse the model and find-

(i) Deflection of nodes on curve C_1 and

(ii) The holding forces of nodes on curve C_2 .

(5) Release the nodes on curve C_2, find the deflection at C_2. The holding forces of all nodes on curve C_1 in step 3 multiplied by the deflection of same nodes in step 4(i) will give energy released for virtual growth of the crack from C_1 to C_2. Similarly, holding forces of nodes on curve C_2 in step 4(ii), multiplied by deflection of same node in step 5 will give the energy released when crack grows from C_2 to C_3. The Energy Release Rate is given by sum of all these energies divided by crack extension area. This gives overall Energy Release Rate.

For the given dimensions of diameter (2R=183mm), thickness (2t=5.3mm) of the specimen shown in Fig.3.5, the numbers of elements in radial direction are 15, in thickness 4 and 9 in each sector with angle of 45°.

Equation 2.28 is used to determine closed form results for deflection and Eq.2.31 for Energy Release Rate. The data by numerical and analytical processes for the given specimen of Fig.3.5 are presented in Table 3.2 and deflected view of the specimen after FEM analysis is shown in Fig.3.8.

Table 3.2 Deflection and G_I of ECP specimen

Load (N)	Crack Length a (mm)	Analytical δ (mm)	FEM δ (mm)	Analytical G_I (J/m^2)	FEM G_I (J/m^2)
100	a_1=45.0	13.6	14.8	11.73	11.66

Above results shows that there is good matching in δ and G_I by both analytical and numerical methods for ECP specimen.

3.4 CLOSURE

For DCB specimen, there is excellent matching in deflection of load point (δ_{max}) within 2.6% and G_I within 0.5% by FEM and analytical methods. For the ECP specimen, there is reasonably good matching in deflection of centre (δ_{max}) within 9% and G_I within 0.6% by both FEM and analytical methods. The results

match well within 9% from both the methods for isotropic materials. Hence, we can extend this method for noncircular crack fronts for which analytical results are not available in Chapter 4 for composites.

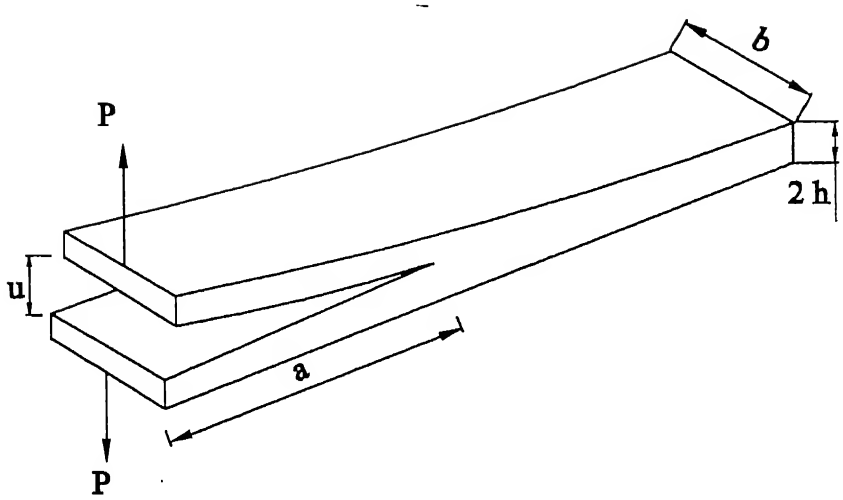

Fig. 3.1 DCB Specimen loaded in mode I.

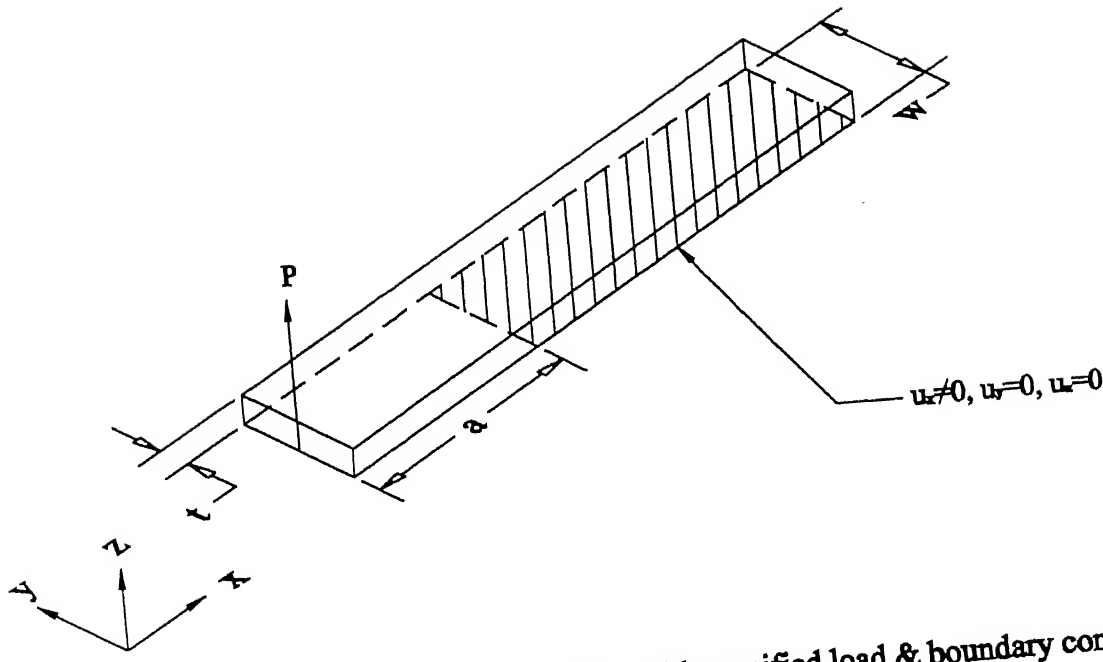

Fig. (3.2) Model of DCB specimen with specified load & boundary conditions

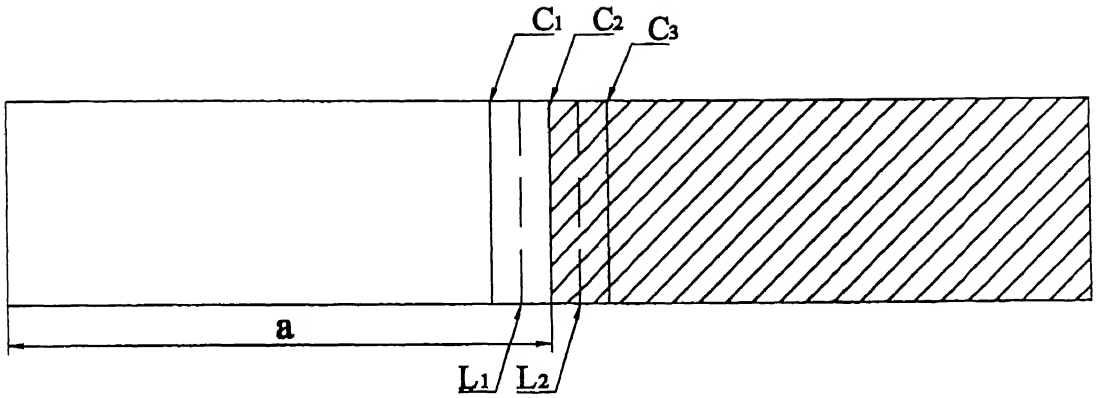

Fig. 3.3 Illustration of MCCI technique

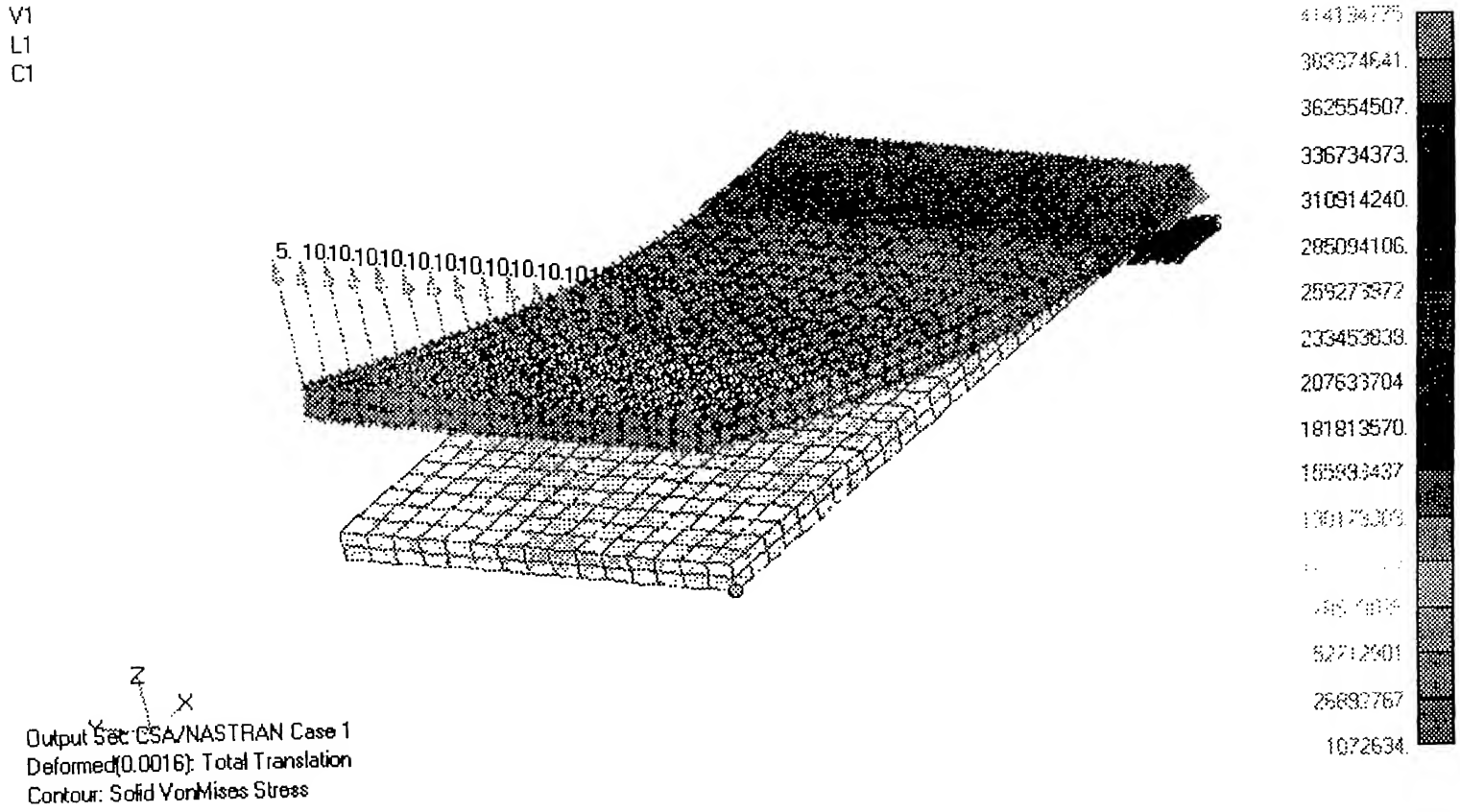

Fig.3.4 Exaggerated view of deflection of DCB specimen

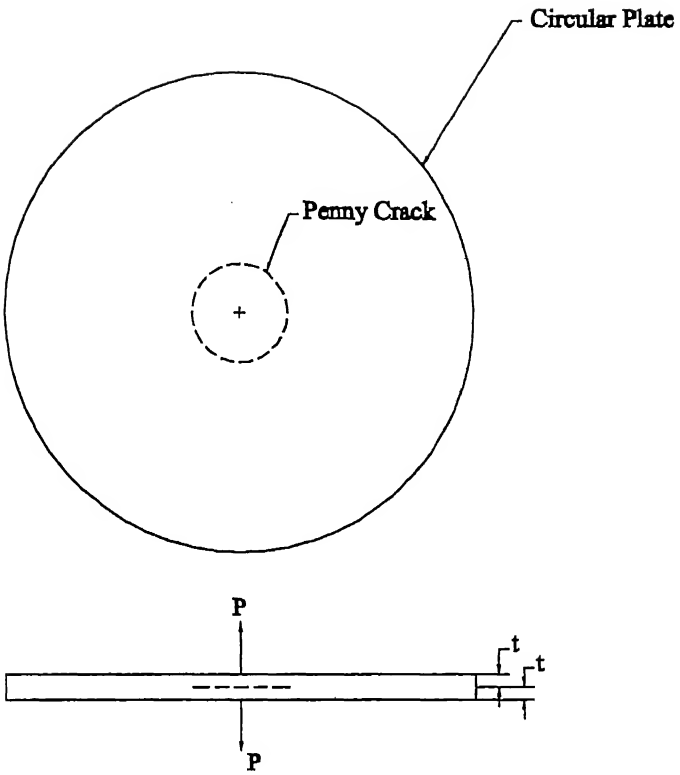

Fig. 3.5 A typical Embedded Crack Plate(ECP) specimen

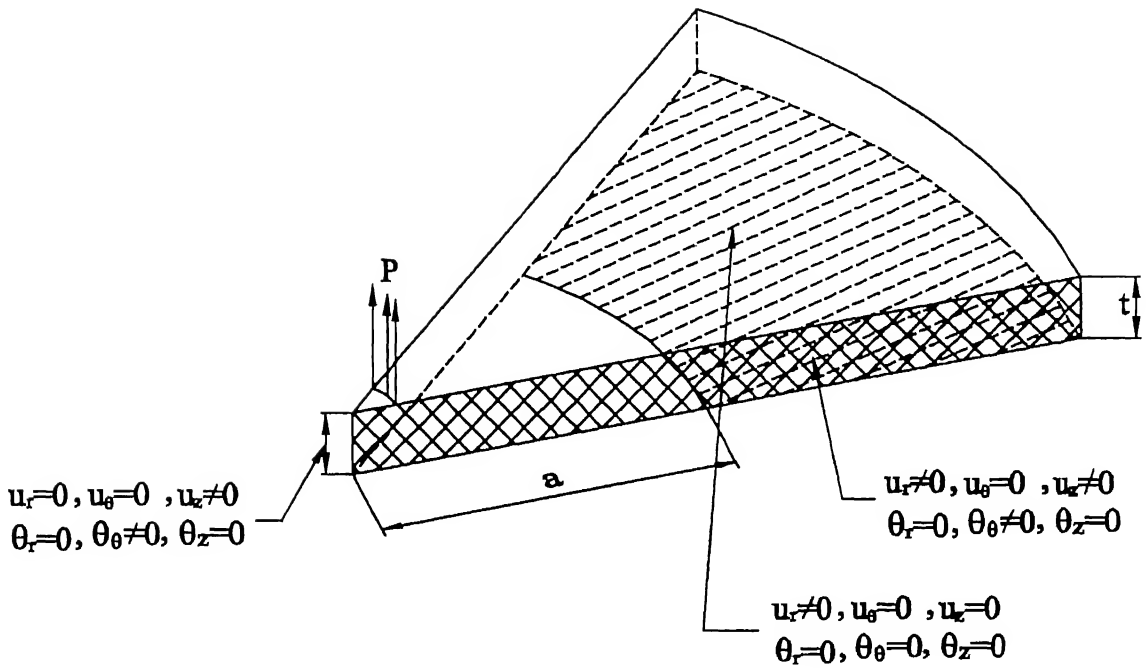

Fig.3.6 One-sixteenth of ECP specimen with specified load and boundary conditions

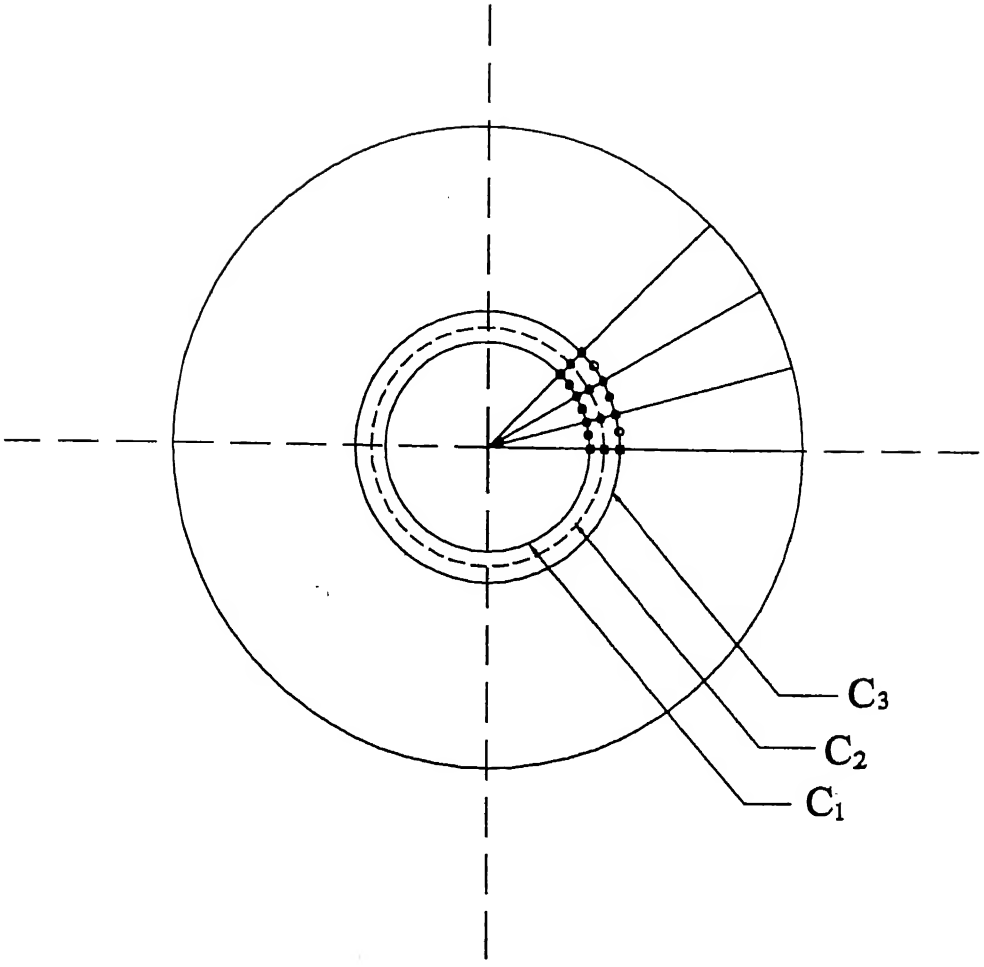

Fig. 3.7 Illustration of VCCI technique in ECP specimen

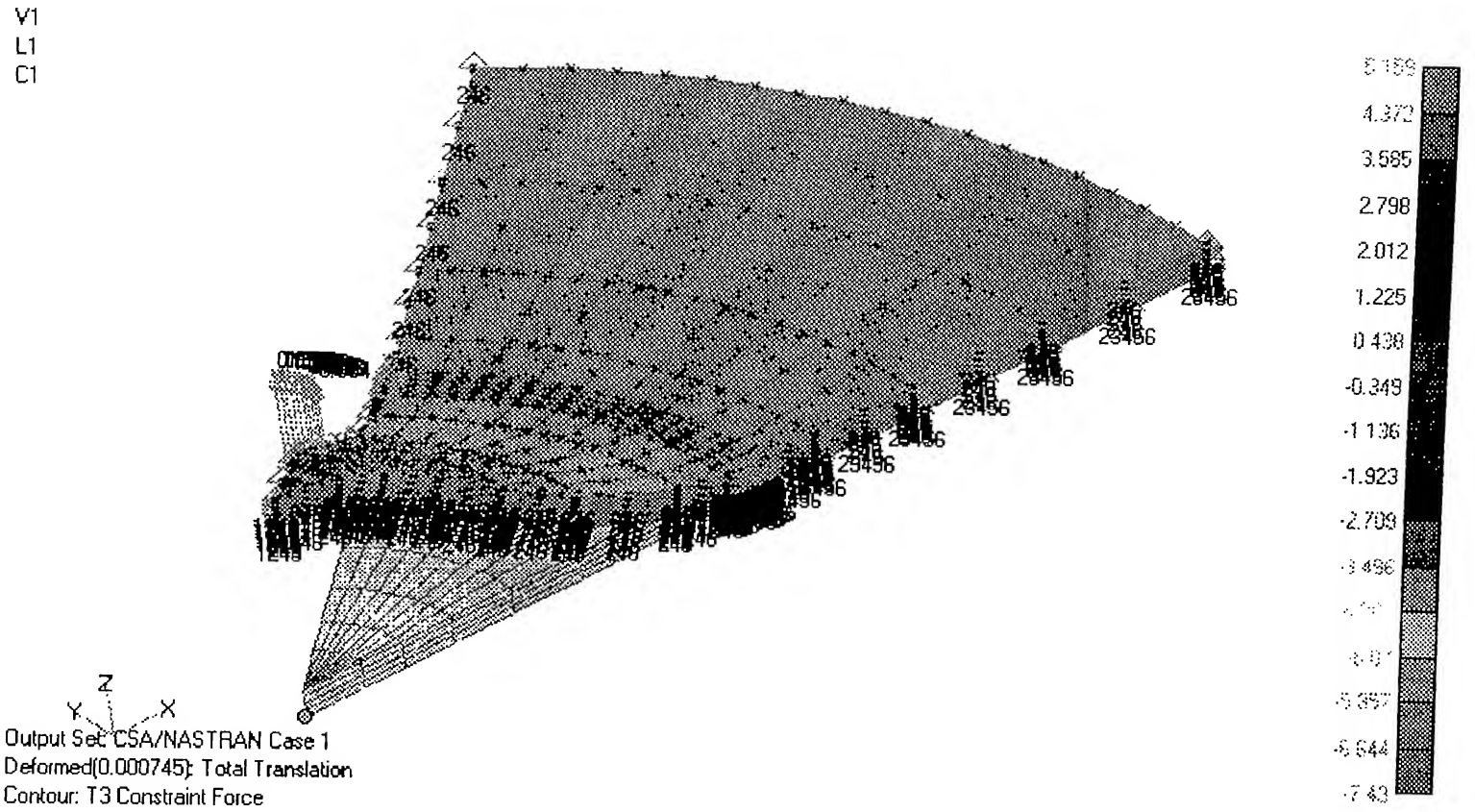
V1
L1
C1
Z
Y
X
Output Set: CSA/NASTRAN Case 1
Deformed{0.000745}: Total Translation
Contour: T3 Constraint Force
4.372
3.585
2.798
2.012
1.225
0.439
-0.349
-1.136
-1.923
-2.709
-3.496
-4.357
-6.644
-7.43

CHAPTER-4

EXPERIMENTAL TECHNIQUE FOR FRP LAMINATES

4.1 INTRODUCTION

Chapter 2 explains the analytical formulations for DCB & ECP specimens to determine the Interlaminar Fracture Toughness. The Experimental-Analytical method is not found to be suitable for anisotropic materials because in anisotropic materials, the crack front for ECP specimen is not circular and analytical closed form solutions are not available.

In this chapter, procedures for Experimental-Numerical technique are discussed to determine the fracture toughness of FRP composites by ECP specimens. The model of the experiment is created on FEMAP package and analysed with CSA/NASTRAN package. The results obtained with analysis are utilised to determine G_{Ic} of FRP composites. G_{Ic} of FRP composites determined through ECP specimen are compared with the conventional method of DCB specimen of same composite laminate.

4.2 EXPERIMENTAL PROCEDURE

4.2.1 SPECIMEN PREPARATION

In the present work, we are mainly focussing our attention on glass fabric/epoxy laminate. Specimen preparation starts by employing prepreg tapes, which are prepared on Unidirectional Prepreg Machine, developed by Kumar et al. (1995). The fibres used are purchased from CEAT Tyres India Ltd. and woven into fabric. The matrix consists of epoxy LY-556 and hardener HT976 along with accelerator XY73 and silane (to obtain better wetting of fibers) in the weight ratio of 100:35:1.5:0.5. The resin and hardener are purchased from Ciba–Geigy Ltd. Bombay.

ECP Specimen:

ECP specimen of 32 prepreg plies with an embedded penny crack in the mid plane is prepared by laying up laminae (prepreg tapes) at different orientation. In the present work, we have considered following configuration of laminate.

- $[0/90]_{8s}$ Unidirectional laminate
- $[0/+45/-45/90/90/-45/+45/0]_{2S}$ Fabric/Epoxy laminate
- $[0]_{32}$ Fabric/Epoxy laminate

To prepare the specimen, 16 layers with specified orientations are stacked on one teflon sheet and other 16 layers on other. Then in centre a hole of 8mm is drilled to accommodate M8 Counter Sunk Screw (CSK) of head dia 15.8mm along with a steel washer of dia 35mm and thickness 0.7mm. The washer is used to avoid the fibre failure from centre of the specimen while being loaded in mode I. In the head of CSK screw a hole is drilled up to 5-6mm depth to accommodate a pin of diameter 2mm to avoid the misalignment of two load-bearing screws. Now the two stacks are combined with a dowel pin in the heads of Counter Sunk Screws and a teflon sheet of diameter 45mm and thickness 25μm in the centre. It is to be noted that the fibre direction of both the portions at the interface are at 0°. The teflon sheet is inserted to have an embedded precrack in the laminate.

Now the stack is placed in a specially designed fixture (Fig. 4.1) for hot pressing. The two plates of fixture are constrained for their lateral displacement by two diagonally placed dowel pins and placed in the hydraulic press. The pressure and temperature are applied on the fixture by platens of hydraulic press. The curing cycle consists of maintaining the specimen at about 125°C and at normal pressure for about 30-45 minutes. The pressure is slowly increased upto 0.7MPa in an hour and this state is maintained for 3 hours. For post curing, the same pressure is maintained and temperature is increased to 150°C and this state is maintained for 4 hours. After that, the specimen is cooled slowly to room temperature and then marked and cut by power hacksaw into diameter of 220-225mm. We have used the bigger size specimen to avoid the end effects, which has been mentioned as draw back in thesis report of Mr. Jagannath Rao (1997).

DCB Specimen:

DCB specimens are also of 32 layers made of glass fabric with epoxy. The orientation of laminae in the laminate are $[0]_{32}$ & $[90]_{32}$.

To prepare the specimen, 32 layers are laid on a teflon sheet with an edge crack placed in the mid plane by inserting a strip of teflon sheet of 25mm width at one edge. Process of curing is same as described for ECP specimen. The specimen is cut of length 150mm, width 30mm and thickness 4mm. A set of tabs has been used in conjunction with universal joints to attain improved mode I loading. Tabs are square blocks of 30mm wide, 6mm thick and are specially designed such that they can be screwed to the cantilever ends without disturbing the specimen (Fig.4.2). The bottom cantilever is screwed to the tab from top through four corner holes in top cantilever, which has clearance to accommodate the head of the screw and top cantilever is screwed to the tab from bottom in the same way. One end of the universal joint is attached to threaded shank from tab and other end goes in jaw of the tensile testing machine.

4.2.2 TEST PROCEDURE

The test consists of determining the Load-Displacement graph and the crack front profile at different interval of time as the crack grows during the application of load in both the specimens.

ECP Specimen:

During the testing process, the load is applied on the specimen through the specially designed universal joint to avoid the bending effect if any. One end of universal joint being tapped, is screwed to the Counter Sunk screw in the ECP test specimen and the other end is fitted inside the loading jaw of a tensile testing machine (INSTRON-1195) as shown in Fig.4.3.

To determine the critical load vs. displacement diagram, the specimen is loaded in displacement controlled mode. The crosshead speed is selected to be 0.5mm/min. and chart speed to monitor is 10mm/min at full-scale load of 5KN. As the experiment proceeds, the load increases linearly with displacement till the precrack starts growing and the loading curve no longer remains linear.

After some growth of the crack front, the machine is stopped and crack front is marked on the specimen against a light from bright lamp placed below the specimen. The process is continued for six to seven times upto the crack passes throughout the specimen. Thus the data obtained from the tests are:

- the Load-Displacement graph, and
- the crack front profiles.

The data are used as inputs for the numerical analysis to determine G_{Ic} of the composites.

DCB Specimen

This specimen is also tested in displacement controlled mode on INSTRON-1195 machine as shown in Fig.4.4. Before mounting the specimen on machine, both edges of specimen are coated with a white brittle fluid (typewriter correction fluid). Also, thin strips of graph paper are glued on both edges to measure the crack growth. The crosshead speed is selected to be 1mm/min and chart speed as

20mm/min at full scale load of 0.2KN. After the crack grows by 6-7mm, the machine is stopped and the crack is marked on the specimen corresponding to a particular point on Load-Displacement diagram. Then the specimen is unloaded to zero load. Now the specimen is loaded again and the process is repeated 7-8 times, each time with larger crack length. The record of Load-Displacement diagram and crack fronts marked on the specimen are used to calculate G_{Ic} by well-known compliance method discussed in Chapter 2.

4.2.3 FINITE ELEMENT MODELING AND ANALYSIS

Modelling

On the basis of experimental results, the ECP specimen is modelled with the specified crack front, load and boundary conditions. The model is created on FEMAP (version 5) package for static analysis and analysed with CSA/NASTRAN package. For the specimen consisting of 32 layers of lamina, 3D brick elements with 3D orthotropic material properties are used for each lamina. 3D brick elements are used to account the shear deformation of elements in Z-direction. Literatures on FEM & its application related journals (Cook et.al., 1989) report that for thin plates, when number of elements are more in thickness direction, the efficiency of elements reduces due to 'shear locking phenomenon'. Therefore, it is suggested to use reduced integration order. The package has facilities to overcome this error by using 'zero integration network' for reduced integration. Each layer is treated as an orthotropic layer and laminate is modelled as sequence of laminae perfectly bonded together. The bond between two laminae in a laminate is assumed to be perfect, i.e., interface between laminae is infinitesimally thin and not shear deformable. Washer is also modelled with 20-noded brick elements having two elements in thickness direction using isotropic material (mild steel).

It has been found that the crack front profile for isotropic material (plexiglass) is nearly circular (thesis report by S. Ramamohan Reddy, 1996), but in case of composite, the crack front is generally elliptical. The ratio of major axis (2a)

to minor axis (2b) of ellipse varies with lamina sequence in laminate as the crack grows in mid plane.

Crack front obtained during experimentation is modelled as an ellipse and very fine mesh is created near the crack front. Since, we are interested in determining the G_{Ic} value in 0°direction and 90°direction, we refine the mesh radially in these directions as shown in Fig.4.5 for different types of laminate configurations.

Considering the symmetry in loading, material property and geometry in the ECP specimen, only one eighth of the specimen is modelled for the laminates of sequence $[0]_{32}$ and $[0/90]_{8s}$ to reduce the calculation time, but for $[0/+45/-45/90/90/90/-45/+45/0]_{2s}$ sequence, half portion of the specimen is modelled because there is no symmetry in material property about any axis. It is required to provide adequate boundary conditions to account for the symmetry and crack in the model. Boundary conditions provided are shown in Fig.4.6 for all type of laminate configuration used.

The critical load corresponding to the crack front is determined through the experimentation. The Load vs. Displacement graph on tensile testing machine (INSTRON-1195) gives the critical load for a particular crack front profile. Considering the CSK screw as rigid member (made of carbon steel with high yield stress), we apply load on the washer where head portion of CSK screw rests.

Materials:

The material properties used for modelling are listed below.

- For unidirectional angle ply laminates (The properties $E_1, E_2, \nu_{12}, G_{12}$ are taken from Ramakrishna, 1997 and rest are deduced following the procedure by Chyanbin Hwe et al., 1992 and A.S.D. Wang, 1989)

  E_1=42 GPa ν_{12}=0.25 G_{12}=3.5 GPa

  E_2=6.8 GPa ν_{23}=0.25 G_{23}=3.5 GPa

  E_3=6.8 GPa ν_{13}=0.25 G_{13}=3.5 GPa

- For fabric laminates (The properties are taken from Padamaja, 2000)

  E_1=26.0 GPa ν_{12}=0.21 G_{12}=3.5 GPa

  E_2=11.7 GPa ν_{23}=0.21 G_{23}=3.5 GPa

E_3=6.8 GPa ν_{13}=0.21 G_{13}=3.5 GPa

- For steel washer

E=207 GPa ν=0.3 G=79.6 GPa

ANALYSIS

The model file created in pre-processor (FEMAP) is filename.mod. When this file is exported to CSA/NASTRAN, a data file is created as 'filename.dat'. This data file contains the full information for simulation. The FE code is executed on the basis of this data file. The result obtained is in the form of 'filename.f06'. The result obtained is visualised in the post processor (FEMAP).

To determine the G_{Ic} value by VCCI technique, we determine the constraint forces at nodes on crack front in the first pass. In the second pass, we free the nodes at crack front and let the crack to move to mid nodes. We simulate the problem and determine the displacement of the previous nodes freed and constraint force at mid side nodes. In the third pass, we free the mid nodes and let the crack to move to the edge of the elements and determine the deflection of mid nodes. Using the Eq.(2.37), we can determine G_{Ic} in any direction with reference axis. The process is shown in Fig.2.6 & 2.7.

4.3 CLOSURE

This chapter deals with preparation of ECP and DCB specimens, method of testing, and data reduction for determining G_{Ic}. VCCI technique is used for ECP specimen.

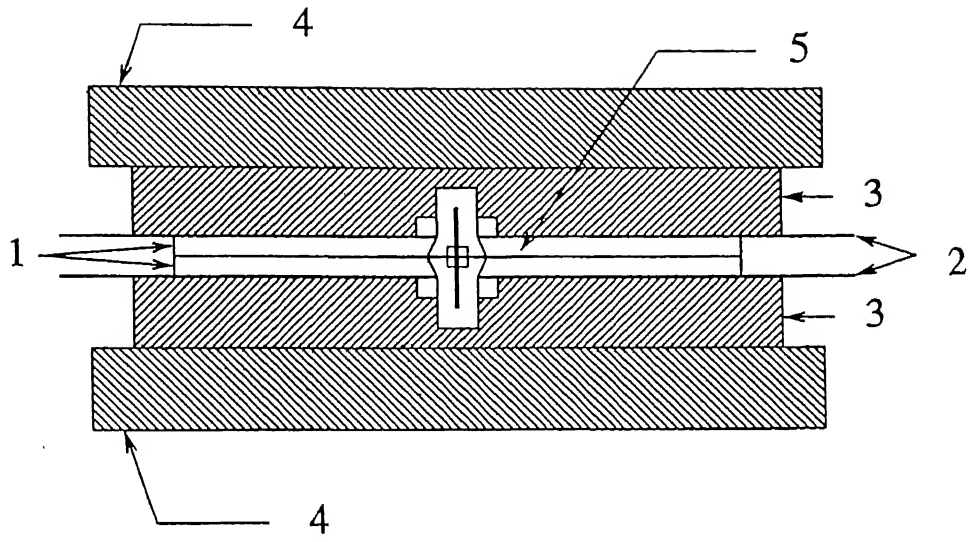

1. Specimen Plates
2. Release films (Teflon)
3. Die Platens
4. Platens of Press
5. Precrack

Fig.4.1 Attachment to prepare ECP specimen.

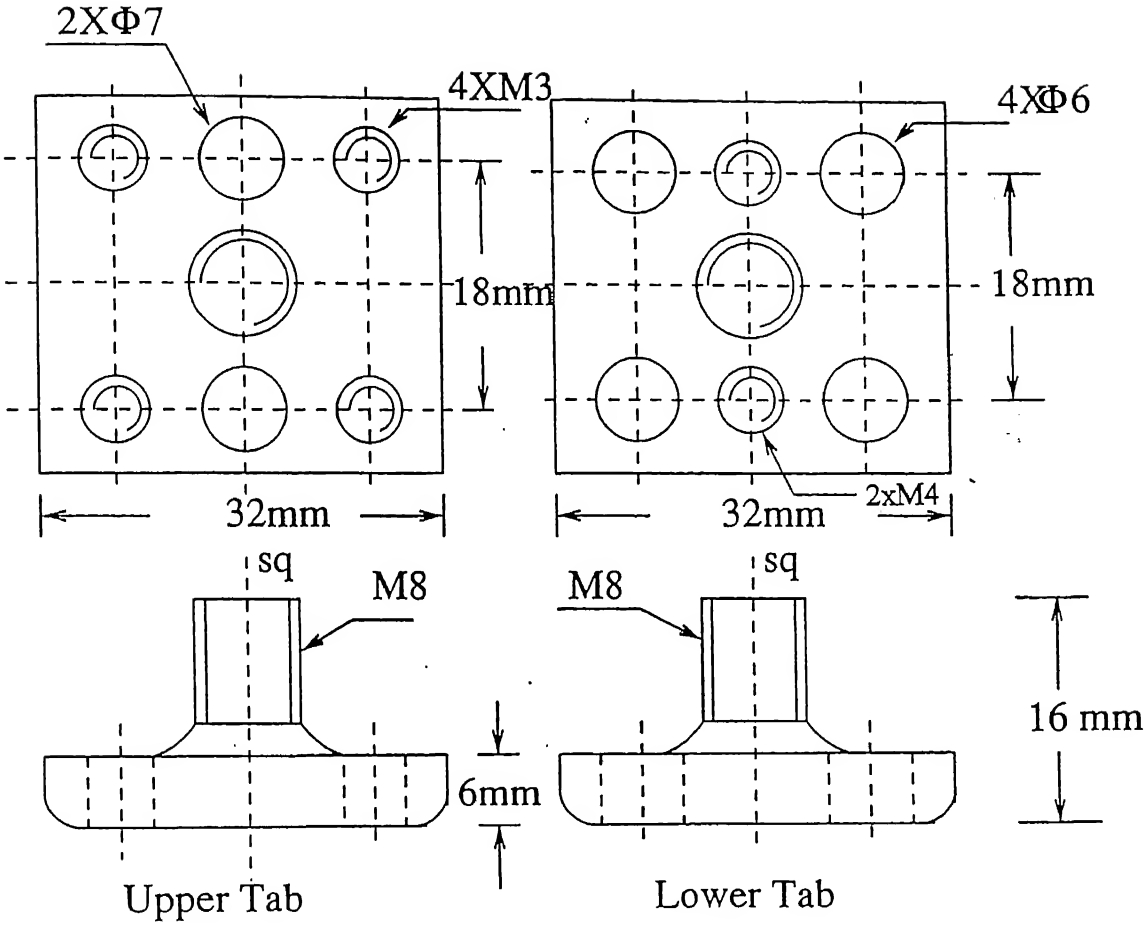

Fig.4.2 Details of Tabs for DCB specimen.

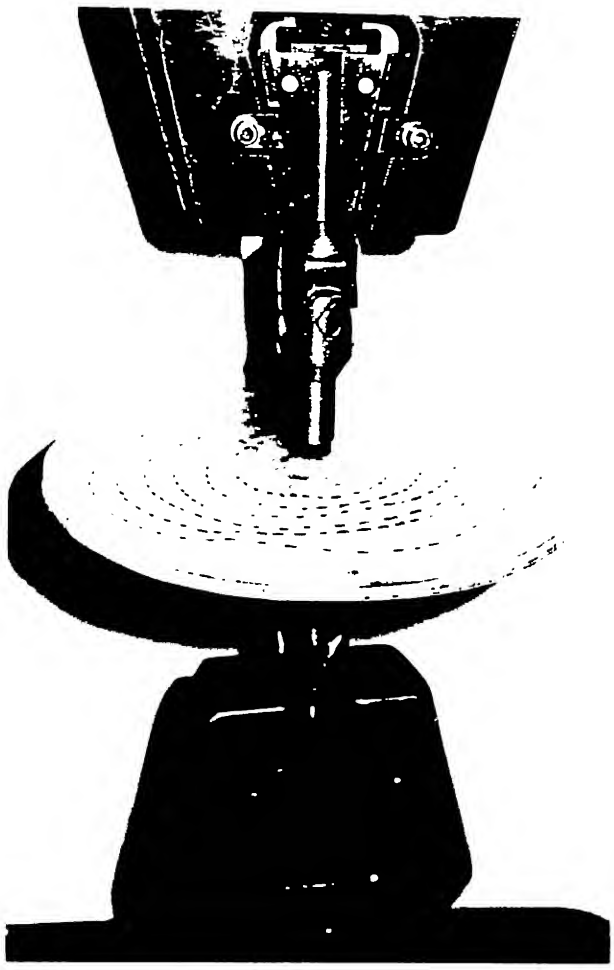

Fig.4.3 Photograph showing ECP specimen loaded in mode I

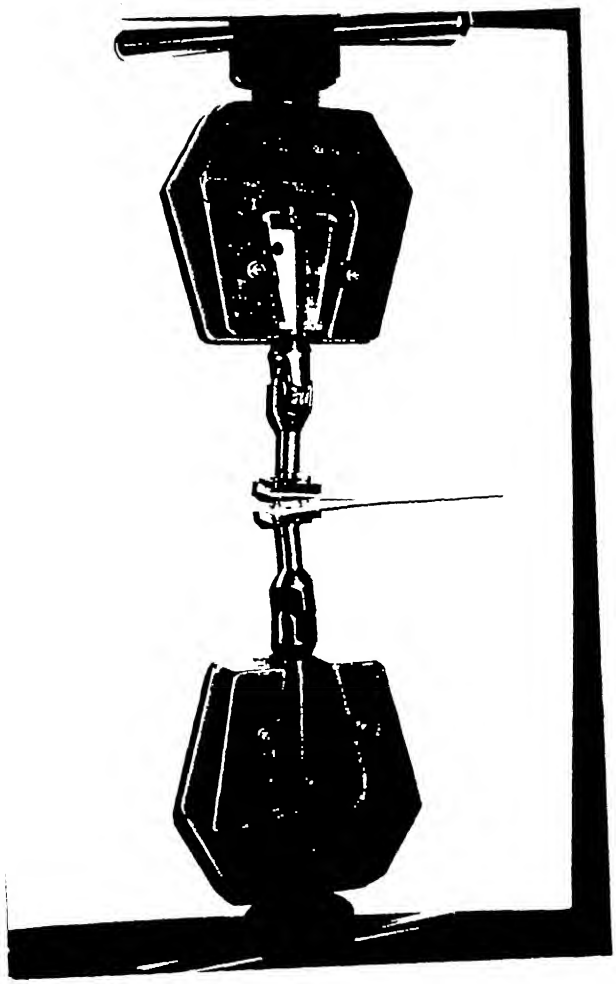

Fig.4.4 Photograph showing DCB specimen loaded in mode I

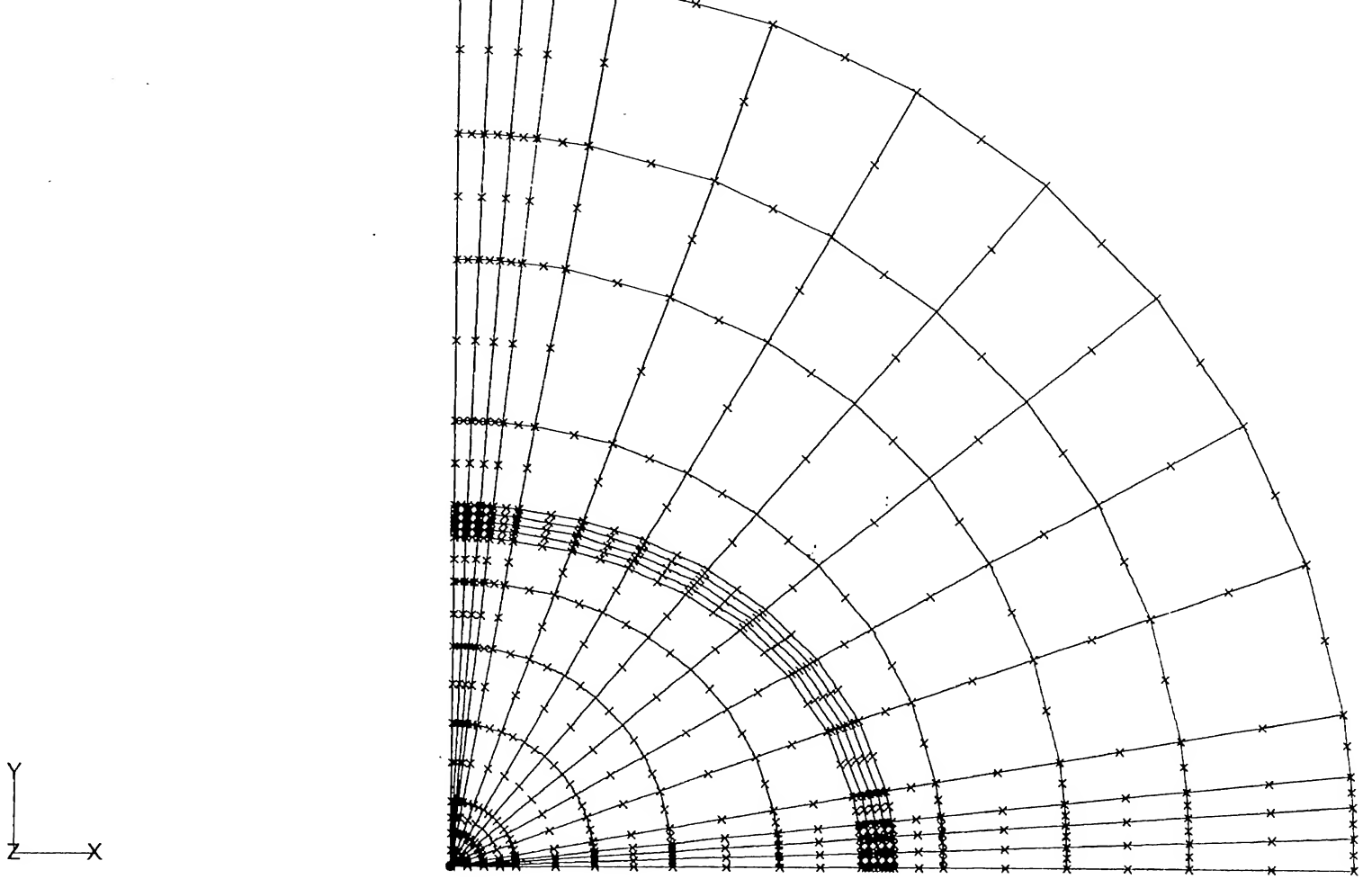

Fig.4.5(a) Mesh configuration to show finer mesh in 0° and 90° for laminates of $[0]_{32}$ and $[0/90]_{8s}$ sequence.

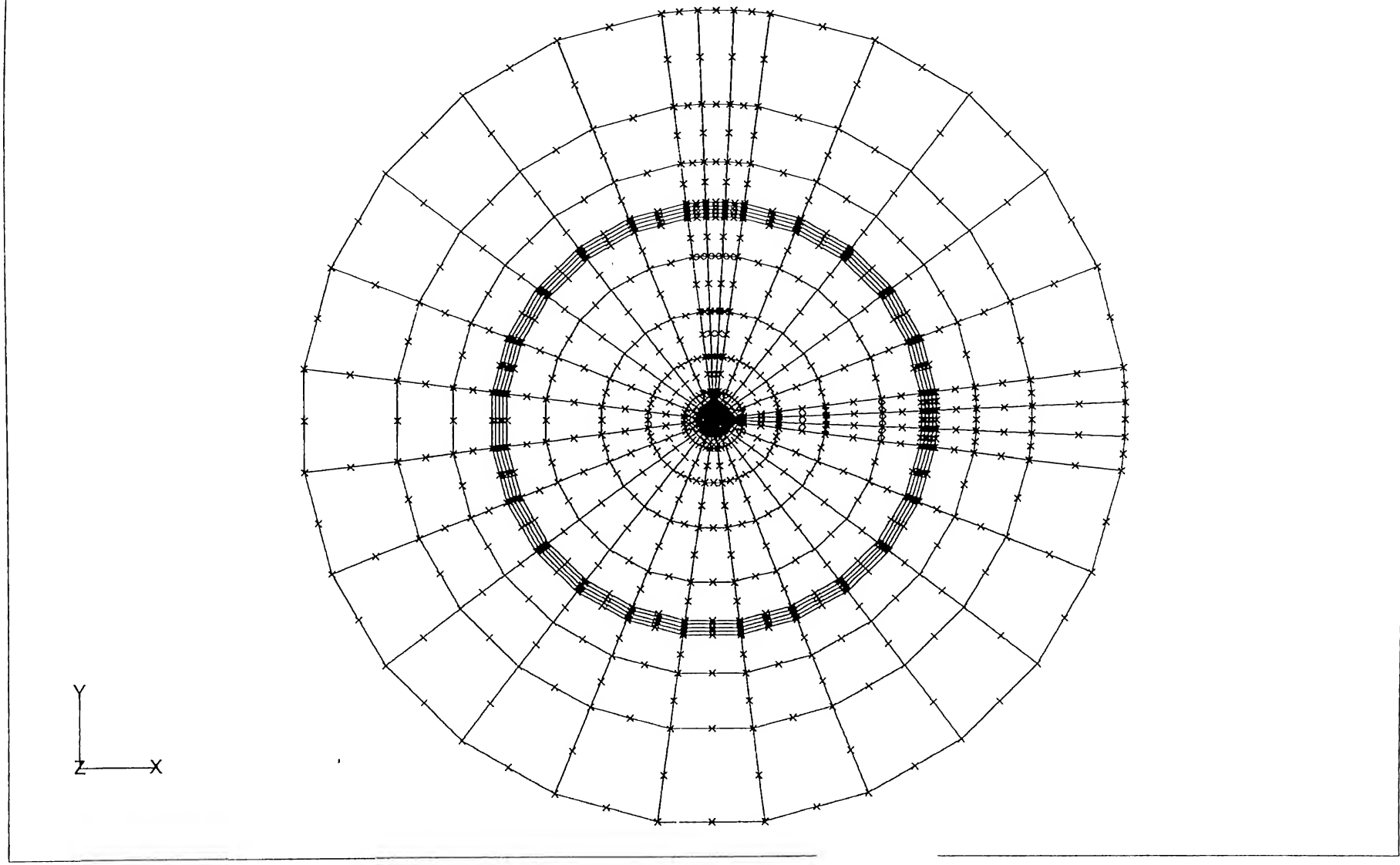

Fig.4.6(b) Mesh configuration to show finer mesh in 0° and 90° for laminate of $[0/45/-45/90/90/-45/45/0]_{2s}$ sequence

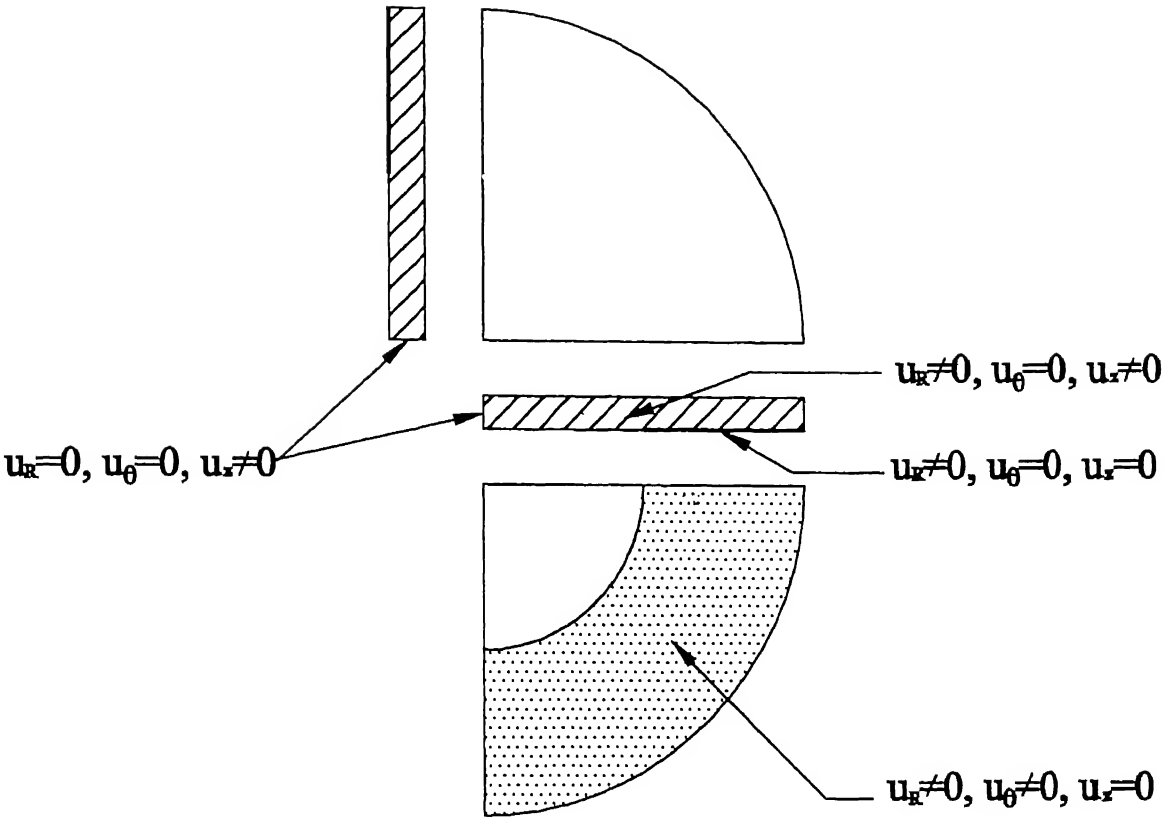

Fig. 4.6(a) Boundary Conditions for $[0]_{32}$ & $[0/90]_{8S}$ Laminates

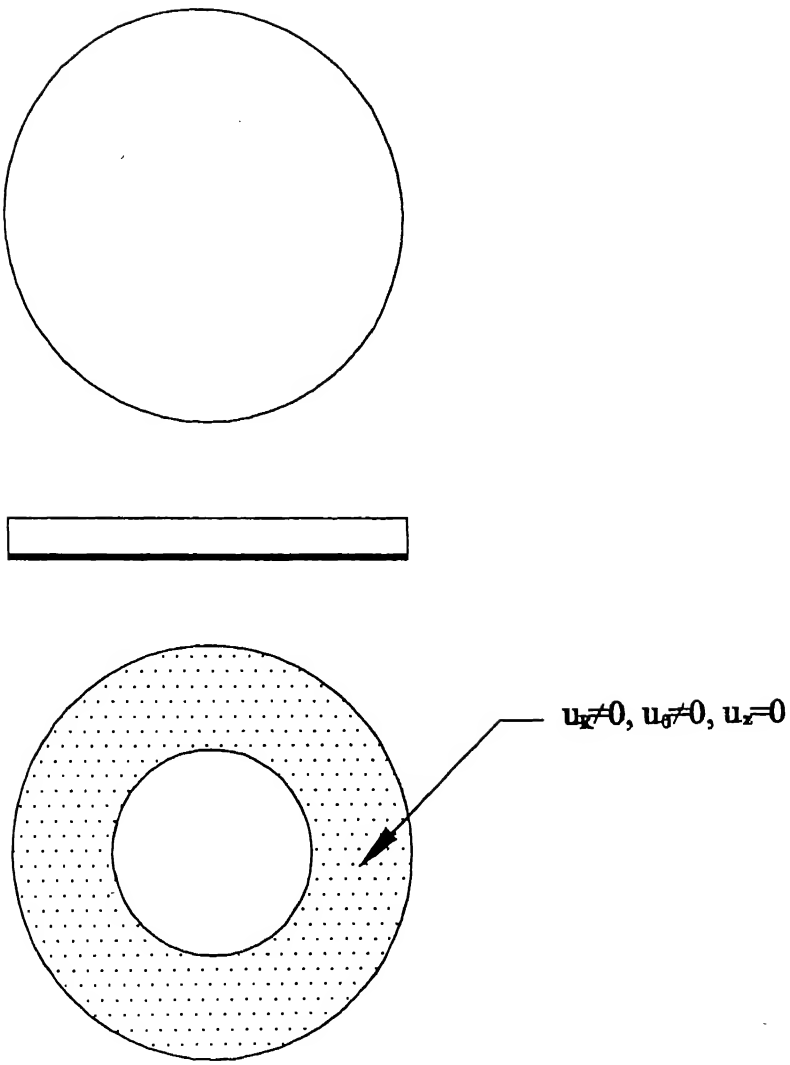

Fig. 4.6(b) Boundary Conditions for ECP specimen of $[0/45/-45/90/90/-45/45/0]_{2s}$ Laminate

CHAPTER-5

RESULTS & DISCUSSIONS

5.1 INTRODUCTION

Tests to determine Interlaminar Fracture Toughness of composite laminates in mode I loading are carried out with ECP specimens and their results are verified with conventional DCB specimens.

During experimentation, specimen geometry, crack profile and critical loads are recorded and used for analysis. The specimens of composite laminates with different configurations are used for testing the crack growth behavior. In this work, three types of laminates are used:

- $[0/90]_{8s}$, glass fiber reinforced epoxy (Cross Ply Laminate)
- $[0/45/-45/90/90/-45/45/0]_{2s}$, glass fabric reinforced epoxy (Quasi-isotropic Laminate)
- $[0]_{32}$, glass fabric reinforced epoxy.

In this chapter, first the geometrical details of ECP specimen are given for each experiment then the results of Interlaminar Fracture Toughness (G_{Ic}) are presented after analysis. Later on, G_{Ic} of a few ECP specimens are compared with G_{Ic} of DCB specimens of same configuration.

5.2 EXPERIMENTAL RESULTS:

5.2.1 Cross Ply laminate

The specimen, called ECP2 in this study, is made up of unidirectional glass fiber/epoxy laminate with laminae sequence of $[0/90]_{8s}$. Its geometrical details are:

thickness (2t) =5.3mm,

outer diameter (2R) =250mm and

precrack diameter =45mm.

The specimen with the preckack is loaded in the tensile testing machine (INSTRON-1195) with a low pulling rate (0.5mm/min.) under displacement controlled mode. Load vs. Displacement diagram is shown in Fig.5.1 and crack front profiles corresponding to critical loads are presented in Fig.5.2. For the crack front C_2 of specimen ECP2, which is approximated as an ellipse (Fig.5.2), the data is analyzed to find G_{Ic}. The data is processed through FEM using CSA/NASTRAN package as explained in Ch.4. The details and results are presented in Table 5.1.

Table 5.1 Details of ECP2, angle ply specimen with configuration $[0/90]_{8s}$

Major Dia. 2a(mm)	Minor Dia. 2b(mm)	Critical Load (N)	u_{max} (Exp) (mm)	u_{max} (FEM) (mm)	G_{Ic} (0°) (J/m^2)	G_{Ic} (90o) (J/m^2)
112	105	2730	4.76	5.52	882	1470

To have a rough estimate of error through FEM analysis, deflection at the center u_{max}, recorded experimentally, is compared with that obtained through FEM. The FEM result is 16% more than the experimental result. This difference is not considered to be large but can be attributed to the combined effect of several causes:

(1) When the crack grows in ECP specimen, there is vacuum created in the specimen which resists jaw movement.

(2) During the curing of the laminate, the proper pressure is not applied due to a shortcoming in the fixture. It was eliminated subsequently.

(3) In unidirectional glass fiber/epoxy laminate, the crack front does not grow in 90 direction on the plane of precrack but shifts to another layer through transverse cracking which is shown in Fig.5.4. This has not been accounted in FEM analysis. Table 5.1 shows that G_{Ic} is 882 J/m^2 in 0° direction and 1470 J/m^2 in 90° direction. The toughness in 90° direction is highly approximate as the interface was between 0° and 90° plies and not between two 90° plies.

5.2.2 Glass fabric reinforced Quasi-isotropic laminate

The specimen, called ECP5 in this study, is made up of glass fabric/epoxy laminate with laminae sequence of $[0/45/-45/90/90/-45/45/0]_{2s}$. In this specimen, the reinforcement material is glass fabric to remove the shifting of the crack plane during crack growth as found in experiments with cross ply laminate. The geometrical details of the specimen are:

thickness (2t) =5.6mm,
outer diameter (2R) =220mm and
precrack diameter =45mm.

Load vs. Displacement diagram and crack front profiles are obtained following the same procedure and shown in Figs.5.5 and 5.6. For the crack front C_2 in Fig.5.6, details and results are presented in Table 5.2 and deflected view of the full plate after FEM analysis is shown in Fig.5.7.

Table 5.2 Details of glass fabric/epoxy laminate with configuration $[0/45/-45/90/90/-45/45/0]_{2s}$

Major Dia. 2a(mm)	Minor Dia. 2b(mm)	Critical Load (N)	u_{max} (Exp.) (mm)	u_{max} (FEM) (mm)	G_{Ic} (0°) (J/m^2)	G_{Ic} (90°) (J/m^2)
116	108	2650	6.15	6.0	742	1042

The error involved in deflection shows the deflection of center through FEM analysis is 2.4% lower than that of experimental. Analysis shows that G_{Ic} in 90° is 1042 J/m^2 compared to 742 J/m^2 in 0° at crack front C_2. Thus, the interface is tougher in 90° direction compared to 0° direction, which leads to elliptical crack front. Specimen ECP5 having laminae sequence of $[0/45/-45/90/90/-45/45/0]_{2s}$ does not possess material symmetry about any axis, so the whole plate is modeled for analysis which requires considerably high simulation time, approximately nine hours for 5040 elements (20-noded brick elements) on Pentium-III ,96MB RAM with 450MHz.

5.2.3 Glass Fabric/Epoxy laminate of configuration $[0]_{32}$

The specimen, called ECP10 in this study, is made of glass fabric/epoxy laminate with laminae sequence of $[0]_{32}$. After conducting experiments with different kinds of laminate, it is realized that $[0]_{32}$ configuration of glass fabric/epoxy laminate is most appropriate in our analysis because it is homogeneous although the material is anisotropic. Also due to symmetry in geometry, material property and loading, only quater plate can be modeled, hence the data reduction can be done on personnel computer in a reasonable duration. The numerical processing of data takes only 3 hours, which is substantially less than that of the analysis on full plate of quasi-isotropic.

During this specimen preparation, shortcomings have been removed which had led to improper pressing of the specimens during curing. The geometric details of the specimen are:

thickness (2t) =4.0mm,
outer diameter (2R) =220mm and
precrack diameter =45mm.

Loads vs. Displacement graph and crack front profiles are obtained following the usual procedure and shown in Figs.5.8 and 5.9. For the crack fronts C_3 and C_4 in Fig.5.9, details and results are presented in Table 5.3. The deflected view of the

specimens obtained after FEM analysis for crack fronts C_3 and C_4, are shown in Figs.5.10 and 5.11 respectively.

Table 5.3 Details of glass fabric/epoxy laminate of sequence $[0]_{32}$

Crack Front	Major Dia. 2b(mm)	Minor Dia. 2b(mm)	Critical Load (N)	u_{max} (Exp.) (mm)	u_{max} (FEM) (mm)	G_{Ic} (0°) (J/m^2)	G_{Ic} (90°) (J/m^2)
C_3	119.4	92	410	1.77	1.976	50.9	102.4
C_4	145.2	114	450	3.1	3.8	74.7	124.0

Table 5.3 shows that deflection at the centre (u_{max}) through FEM is 11.6% higher than the experimentally obtained result at C_3 and 22.5% higher at C_4. Table 5.3 shows that the Interlaminar Fracture Toughness in mode I (G_{Ic}) along 0° direction is approximately half of that along 90°. Further more as the crack grows, G_{Ic} increases in both the directions.

For comparison, the experiments are conducted on the DCB specimens, which is the present standard of measuring G_{Ic}. Interlaminar toughness is determined in two directions, 0° and 90°. The Load vs. Displacement graph on displacement controlled mode are shown in Figs.5.13-5.17. The G_{Ic} obtained through regression analysis (Appendix-A) is presented in Table 5.4.

Table 5.4 Details and Results of DCB tests on glass fabric/epoxy laminate.

Exp.No.	Laminate Sequence	Width (B) (mm)	Thickness(2h) (mm)	G_{Ic} (J/m^2)	Average(G_{Ic}) (J/m^2)
1	$[0]_{32}$	30.8	4	341	334.6
2	$[0]_{32}$	30.7	4	300	
3	$[0]_{32}$	30.7	4	363	
4	$[90]_{32}$	30.9	4	390	463.5
5	$[90]_{32}$	30.8	4	537	

Comparing the results from Table 5.3 & 5.4, it is important to note that G_{Ic} obtained through ECP specimen along 0° and 90° are considerably lower than the G_{Ic} obtained through DCB specimen of same configuration. If a designer employs G_{Ic}, which is determined through DCB specimen, the structure may be on unsafe side. By the trend of different experiments on ECP specimens, it has been found that, G_{Ic} value increases with crack growth (i.e. reduction in curvature). Hence, we can say that, the specimen possesses less toughness at higher curvature.

DCB specimens are loaded in mixed mode at the free edges during experimentation but in ECP specimens free edges are absent. Hence ECP specimens give more factual G_{Ic} compared to the DCB specimens. Also ECP specimen compared to DCB specimen, models some real life problems like damage due to impact of a foreign body which initiates an embedded crack in the mid plane.

It is worth noting that the interlaminar toughness of glass fiber/epoxy laminate (Cross Ply) and glass fabric/epoxy laminate (Quasi-isotropic) are much higher than the toughness of glass fabric/epoxy laminate of configuration $[0]_{32}$. This is probably due to the fact that the compression fixture in the initial stage of this work was not pressing the specimen properly and there was epoxy rich layer at the interface.

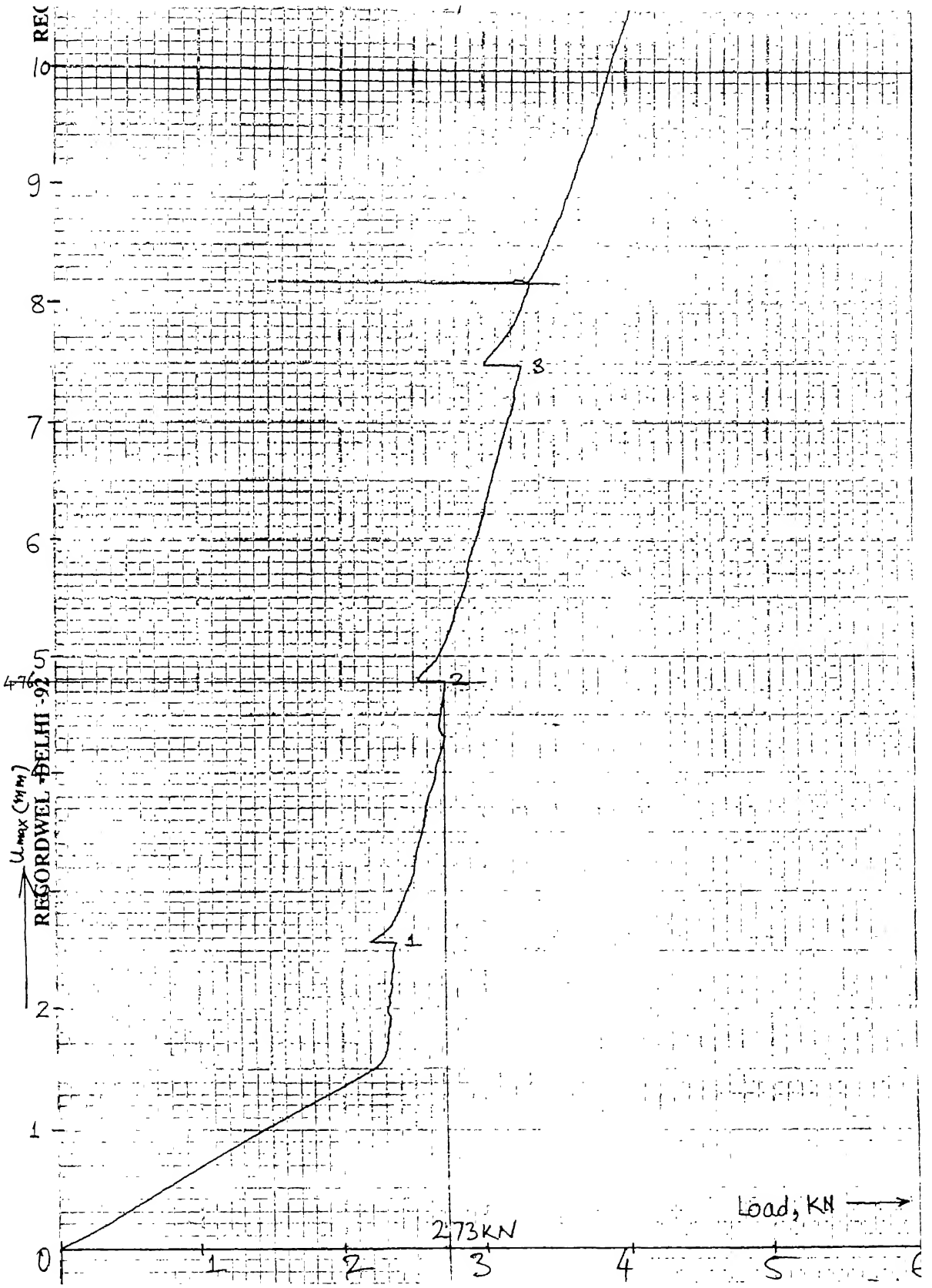

Fig.5.1 Critical Load vs. Displacement graph of ECP2 specimen

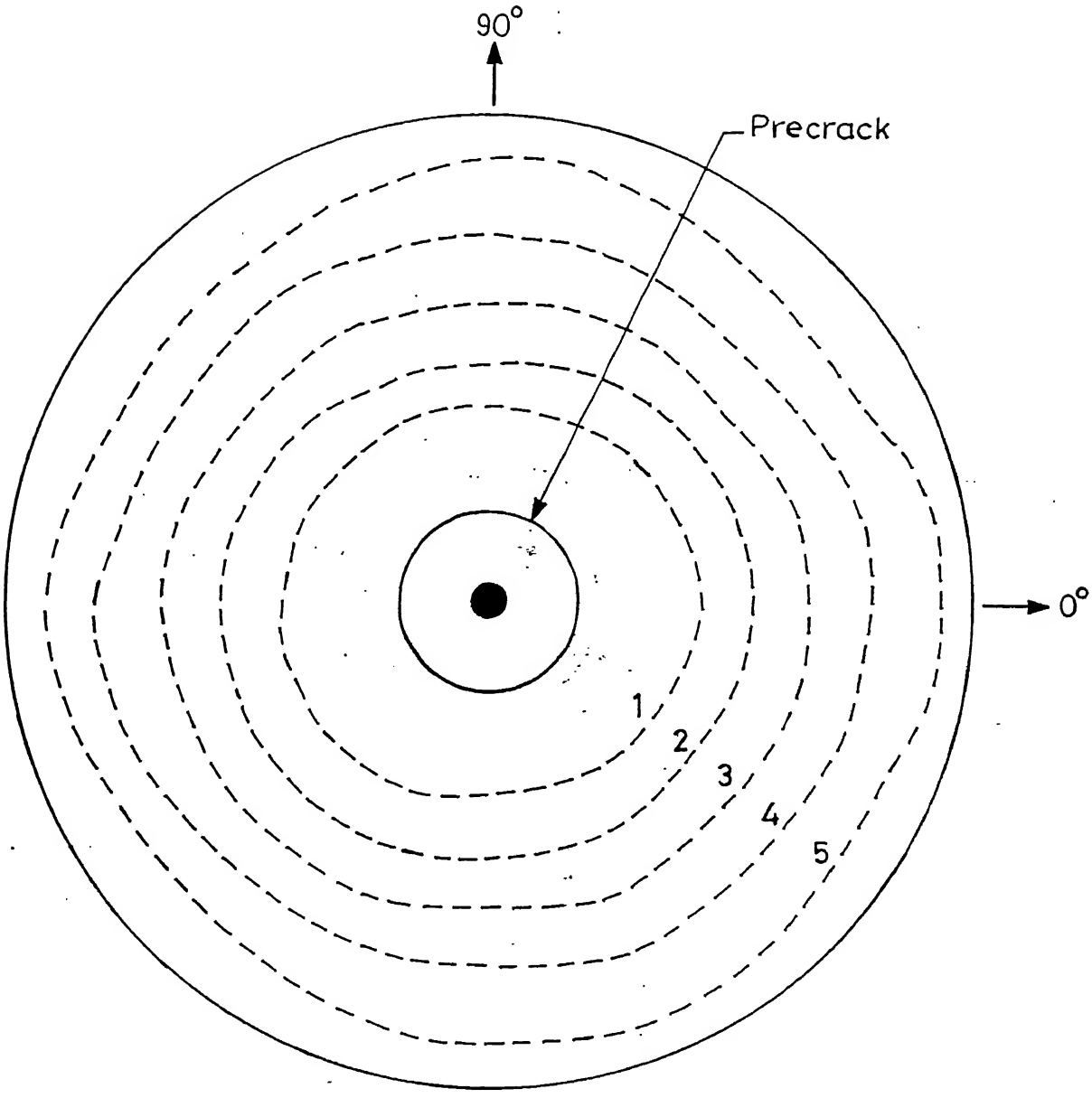

Fig.5.2 Crack front profiles of ECP2 specimen corresponding to Critical Loads

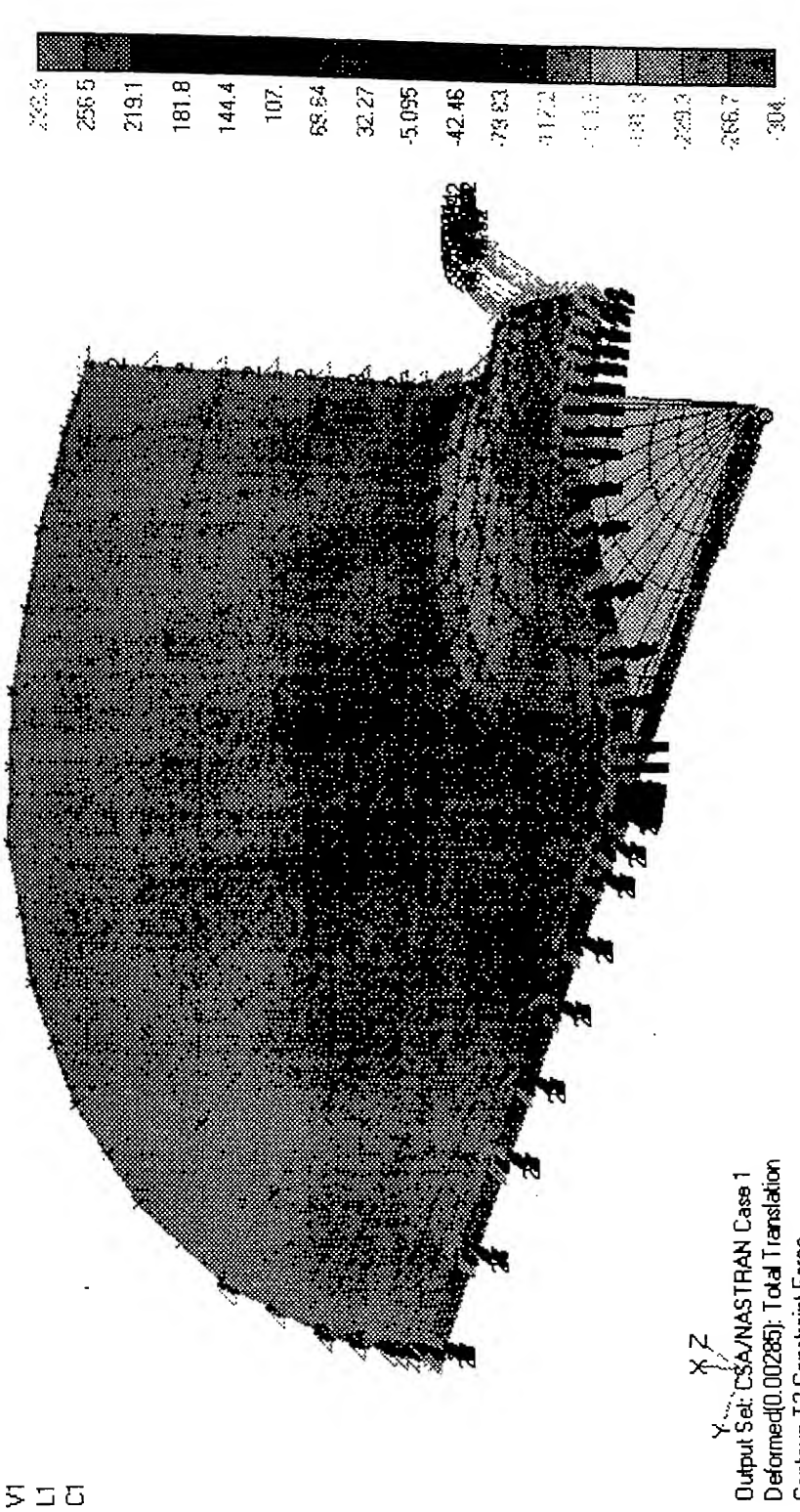

Fig.5.3 Deflected view of ECP2 specimen after FEM analysis

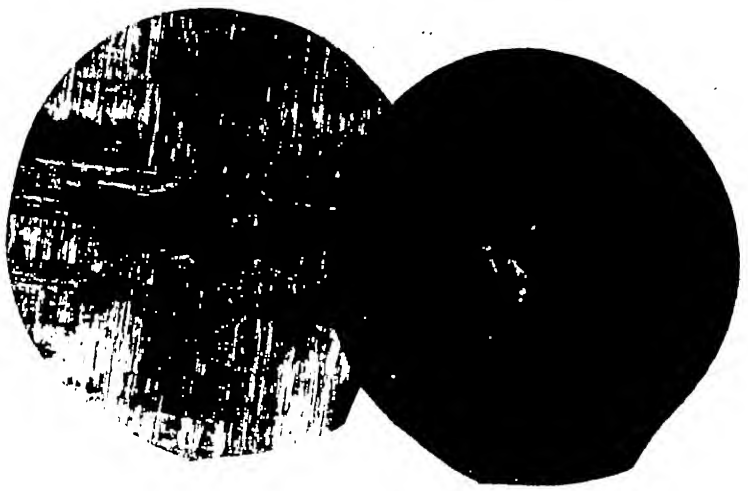

Fig.5.4 Photograph showing Transverse Cracking in Cross Ply Laminate at 90°-90° interface

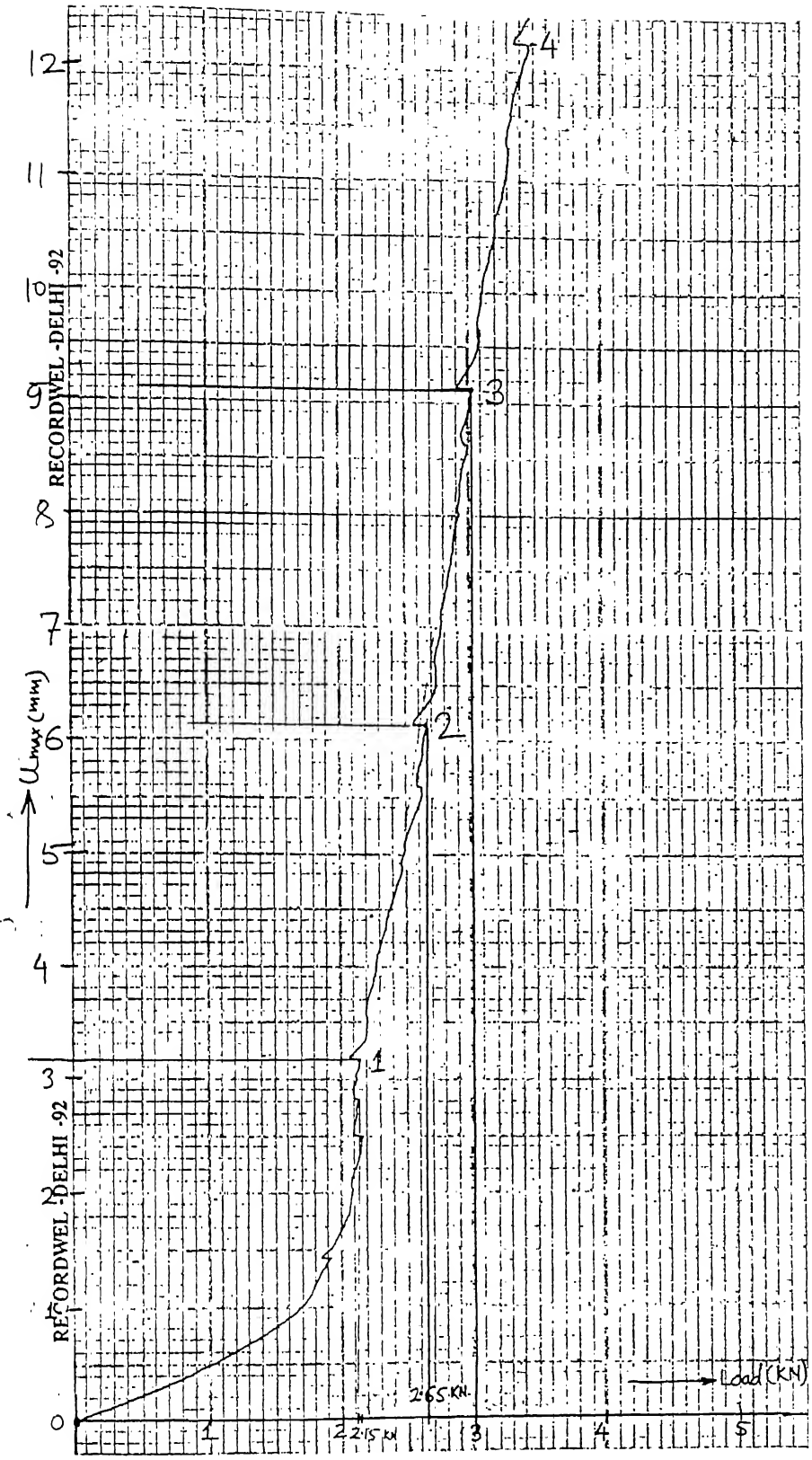

Fig.5.5 Critical Load vs. Displacement graph of ECP5 specimen

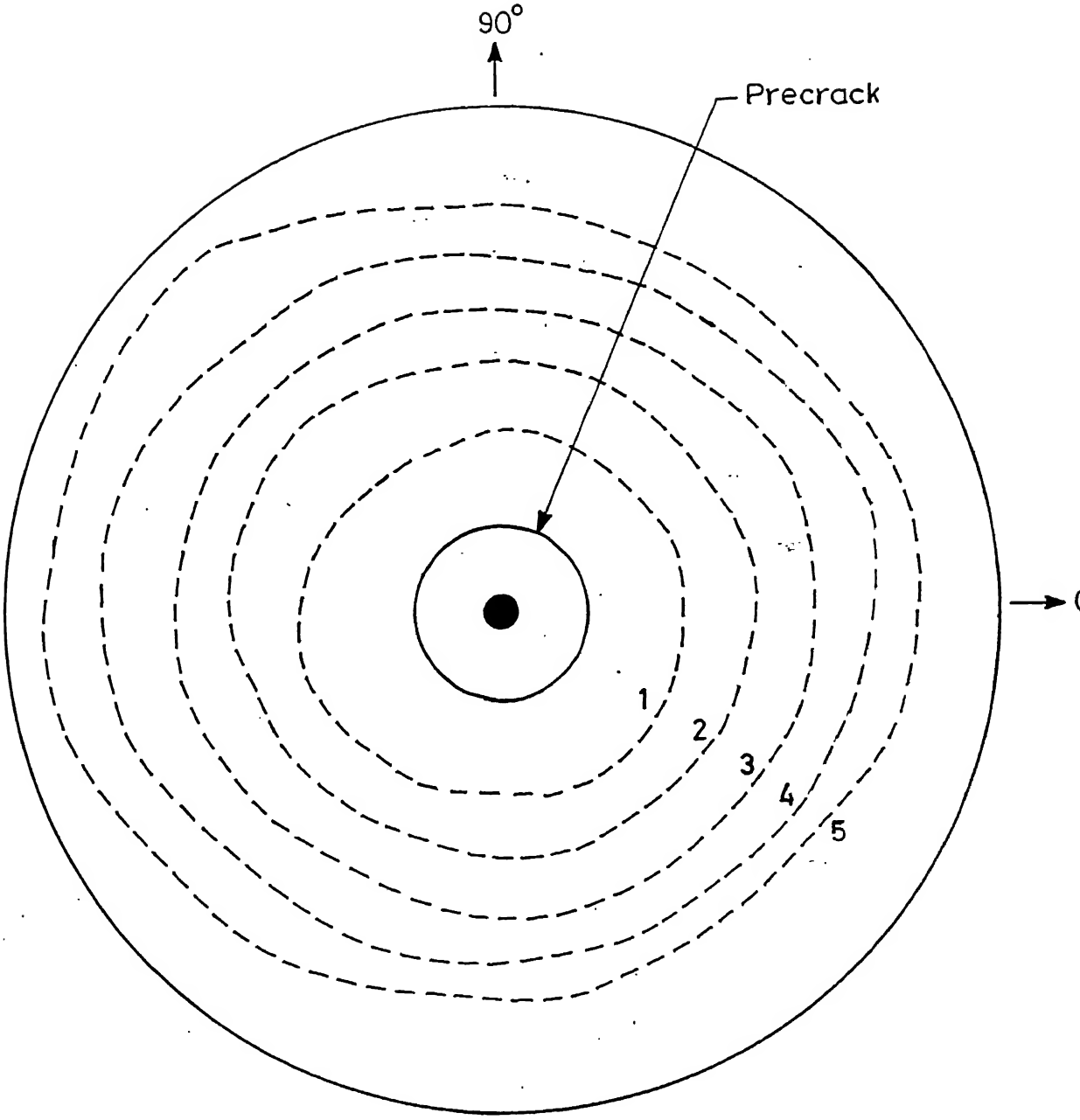

Fig.5.6 Crack front profiles of ECP5 specimen corresponding to Critical Loads

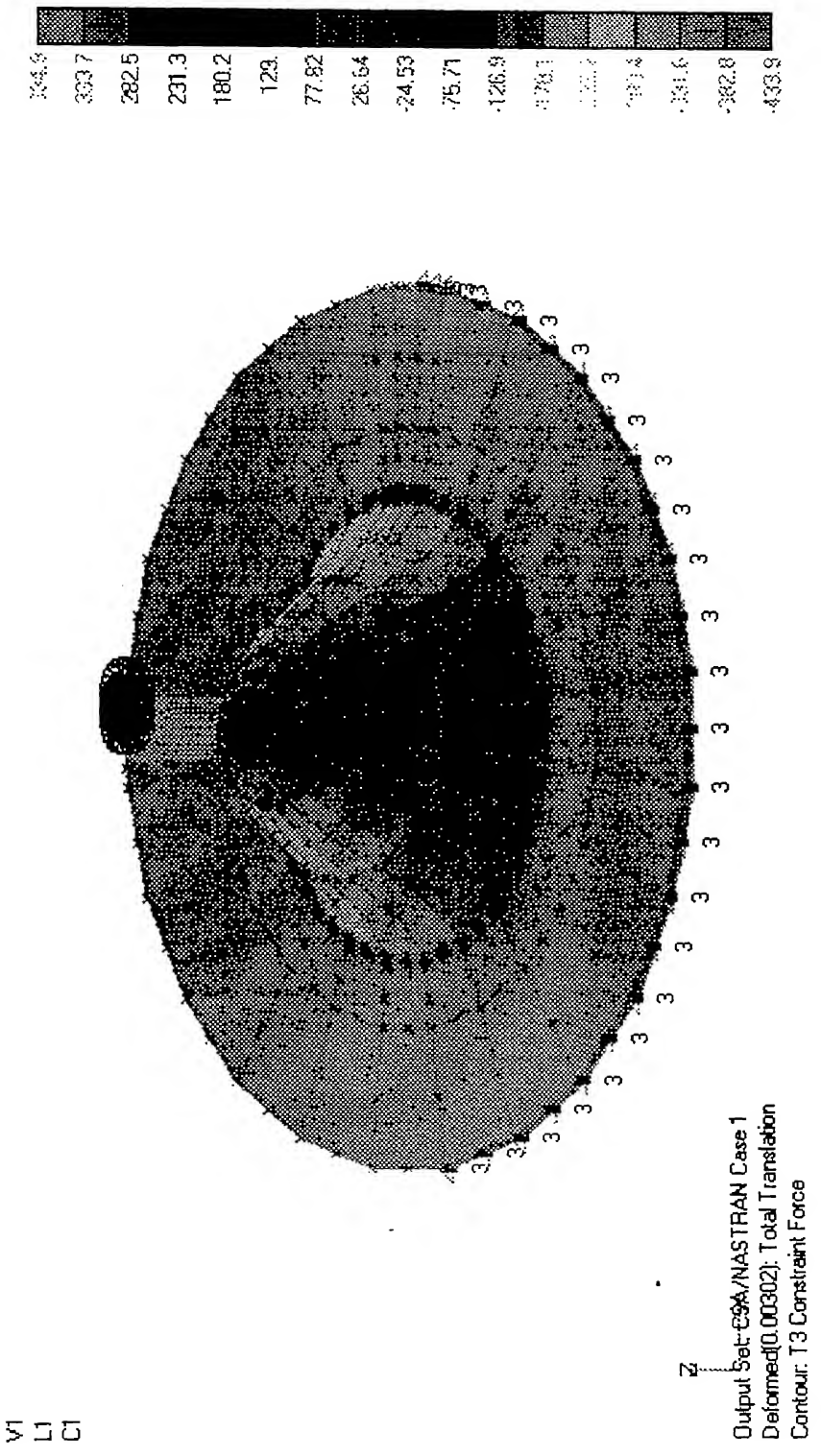

Fig.5.7 Deflected view of ECP5 specimen after FEM analysis

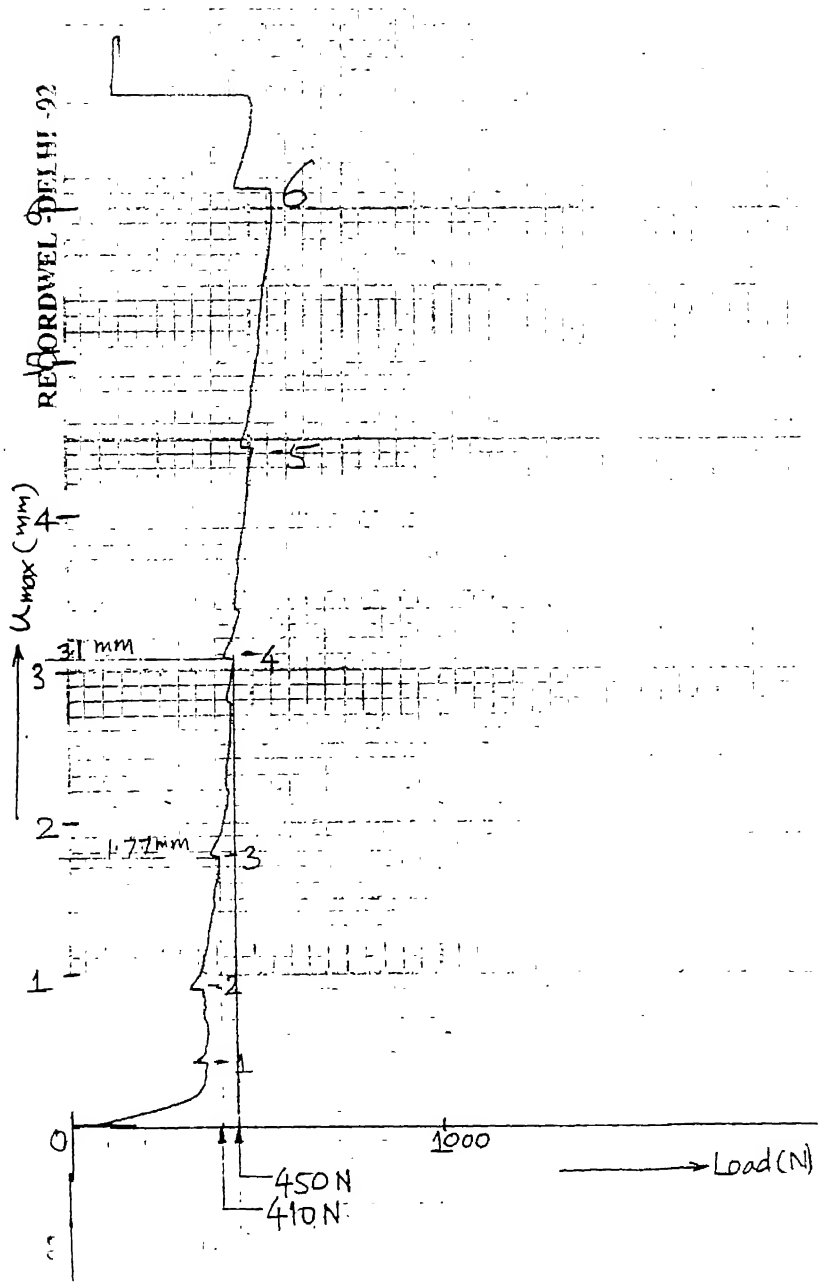

Fig.5.8 Critical Load vs. Displacement graph of ECP10 specimen

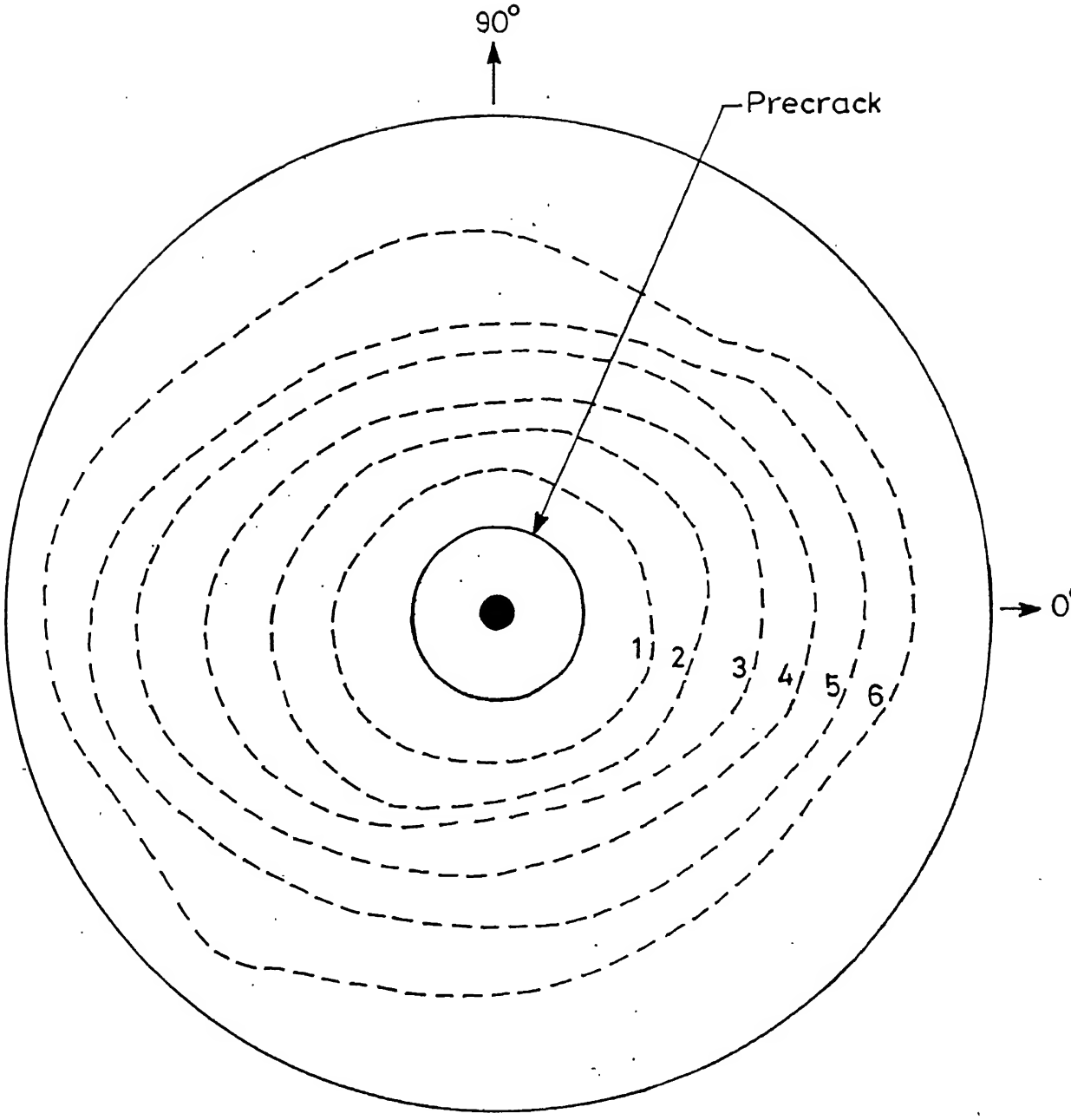

Fig.5.9 Crack front profiles of ECP10 specimen corresponding to Critical Loads

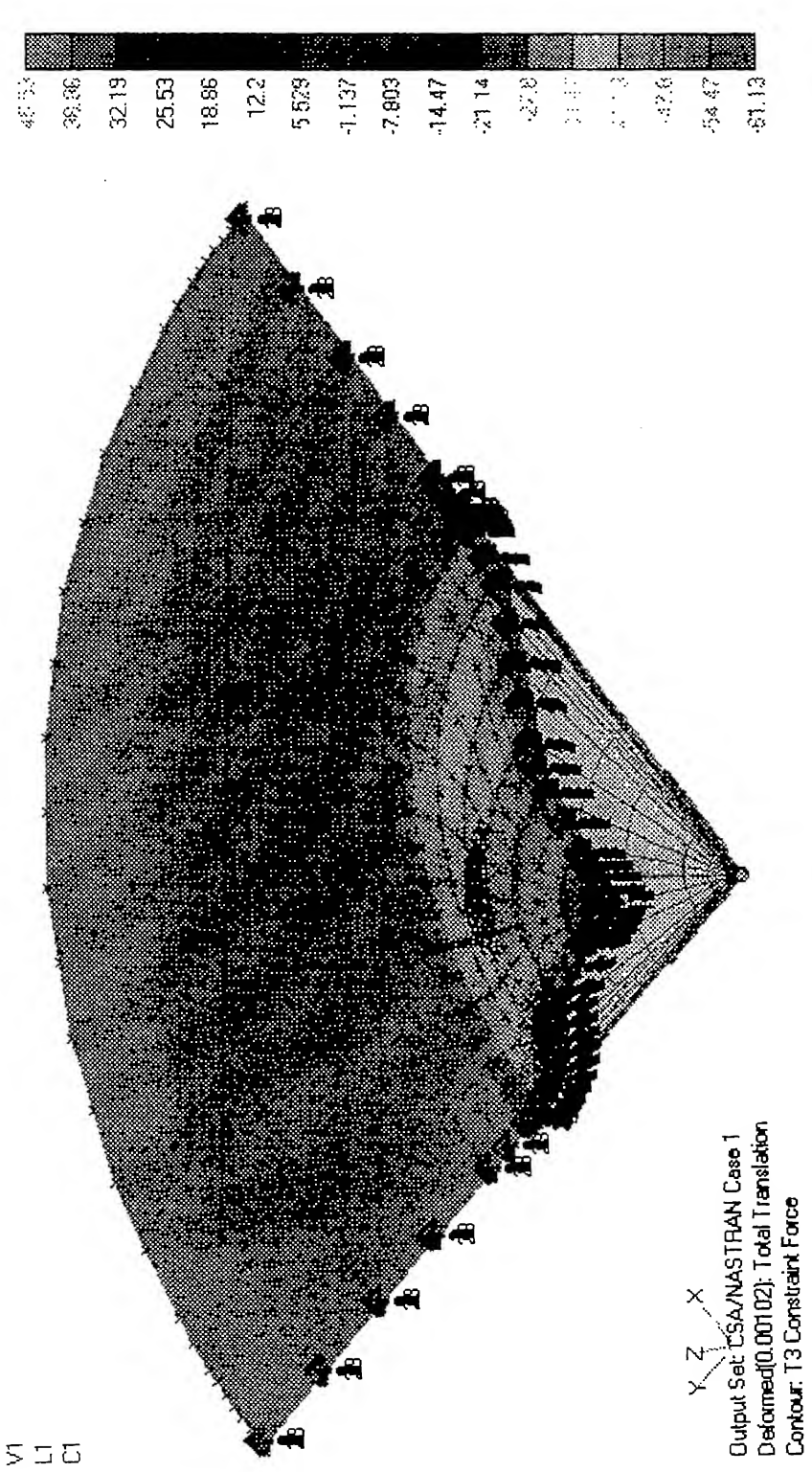

Fig.5.10 Deflected view of ECP10 specimen after FEM analysis at C_3

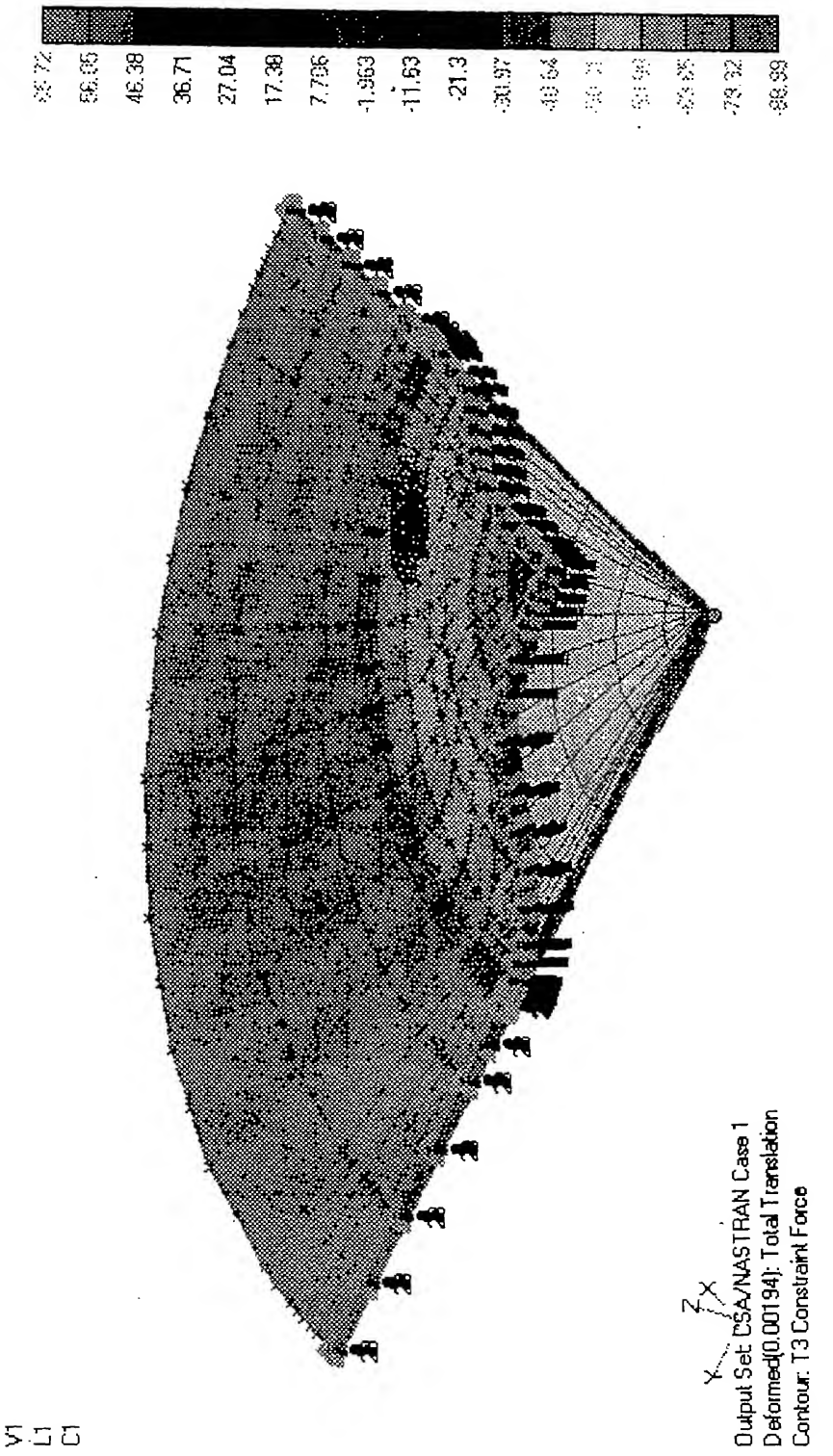

Fig.5.11 Deflected view of ECP10 specimen after FEM analysis at C_4

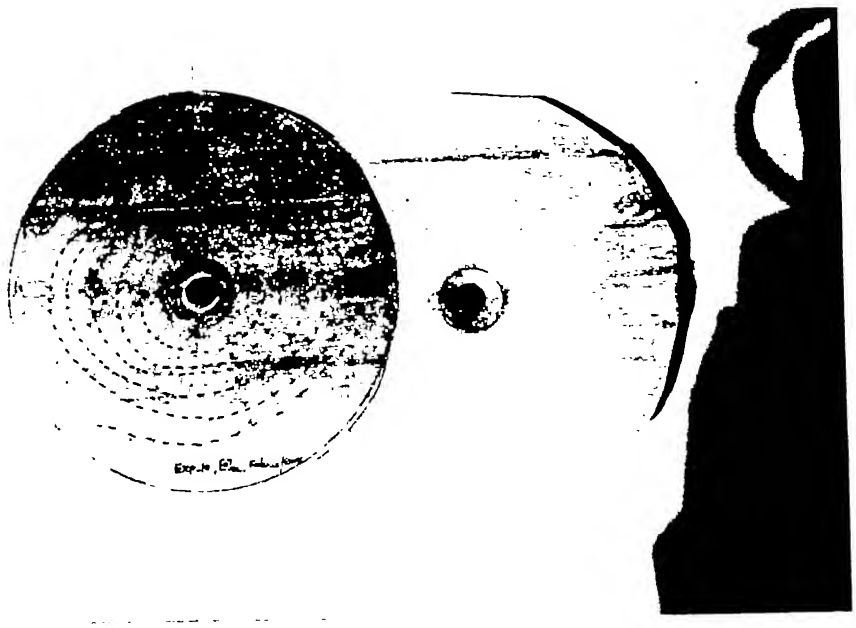

Fig.5.12 Photograph showing separated parts ECP10 specimen

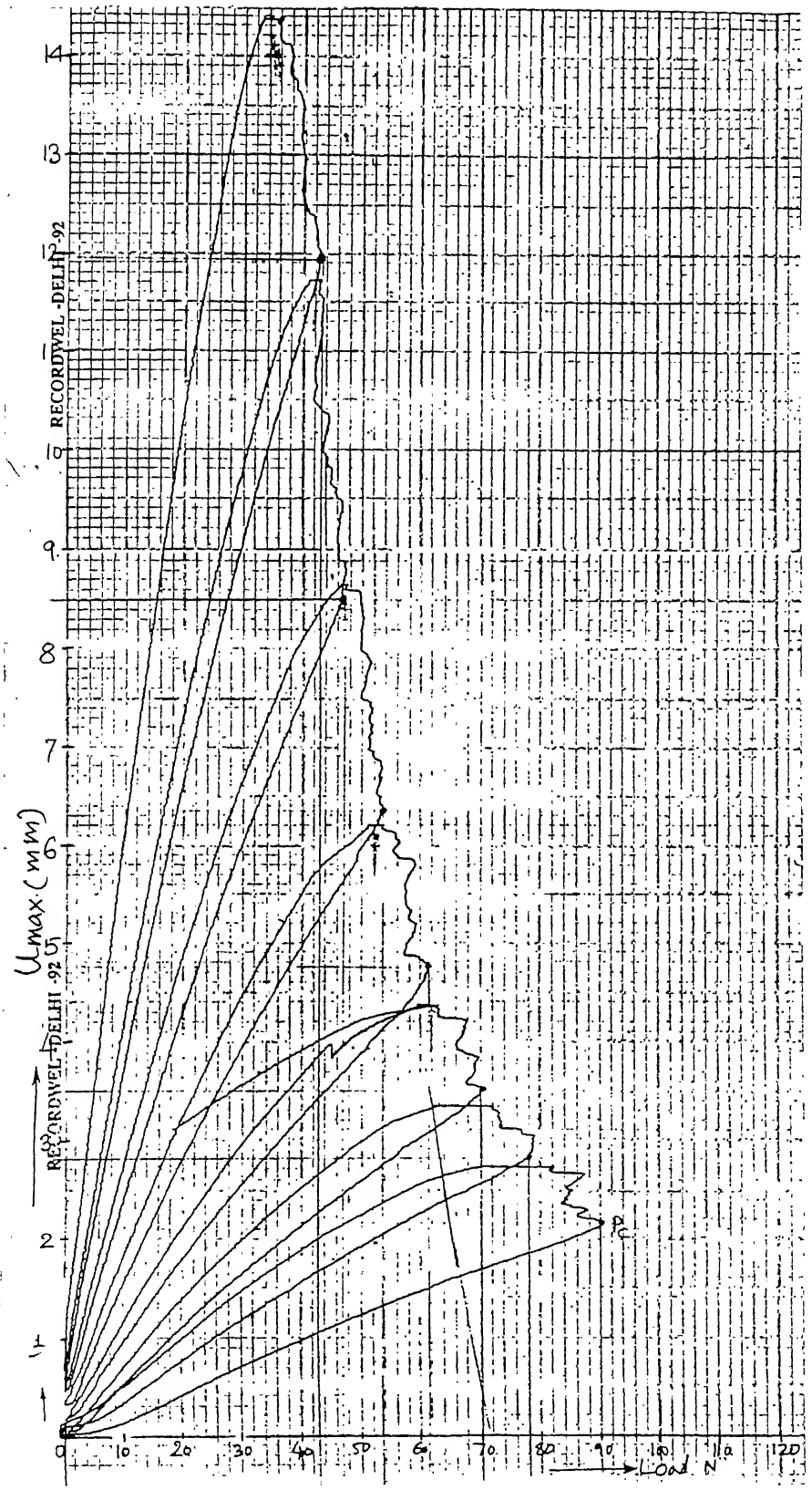

Fig.5.13 Critical Load vs. Displacement graph of DCB specimen (Exp-1)

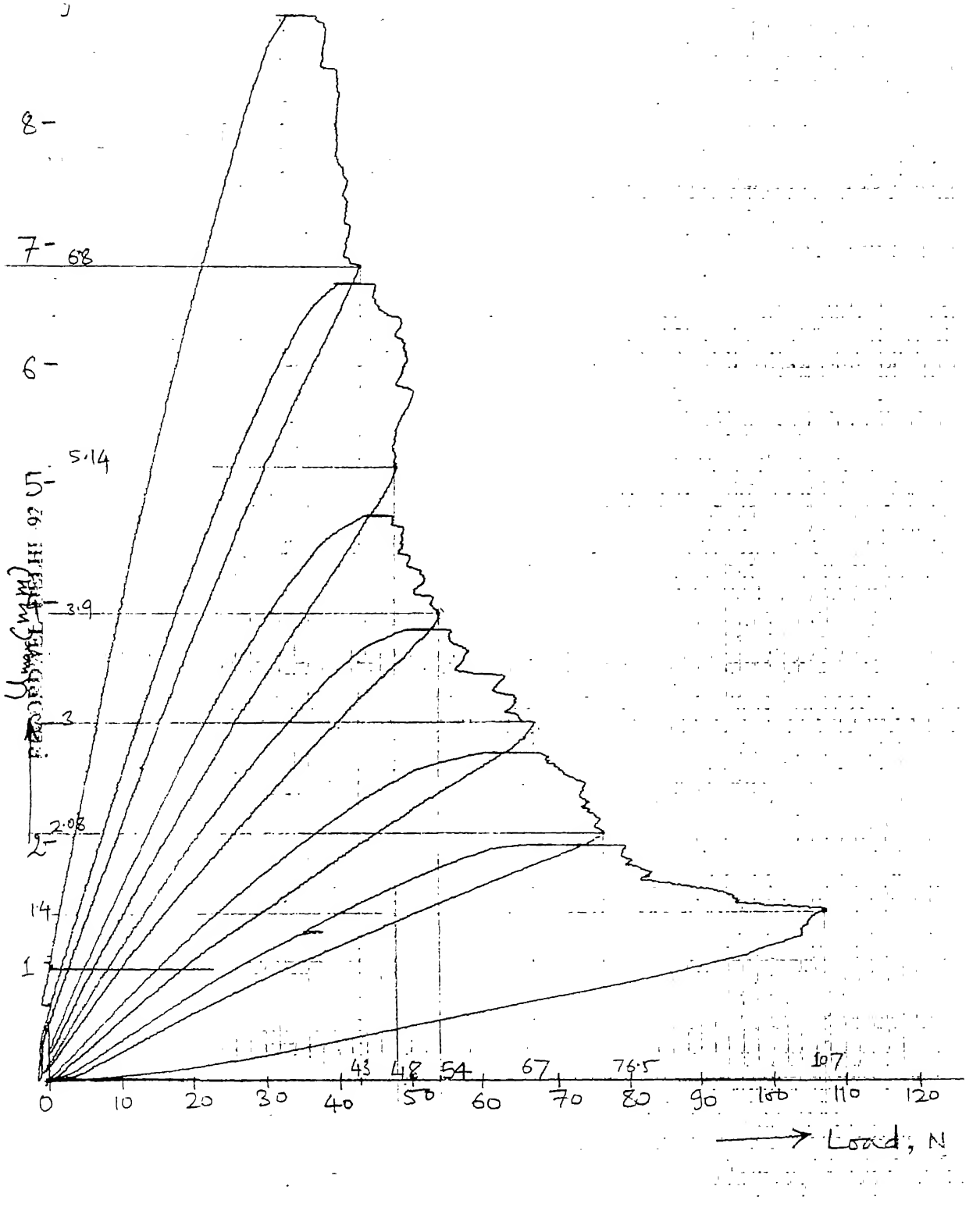

Fig.5.1 Critical Load vs. Displacement graph of DCB specimen(Exp-2)

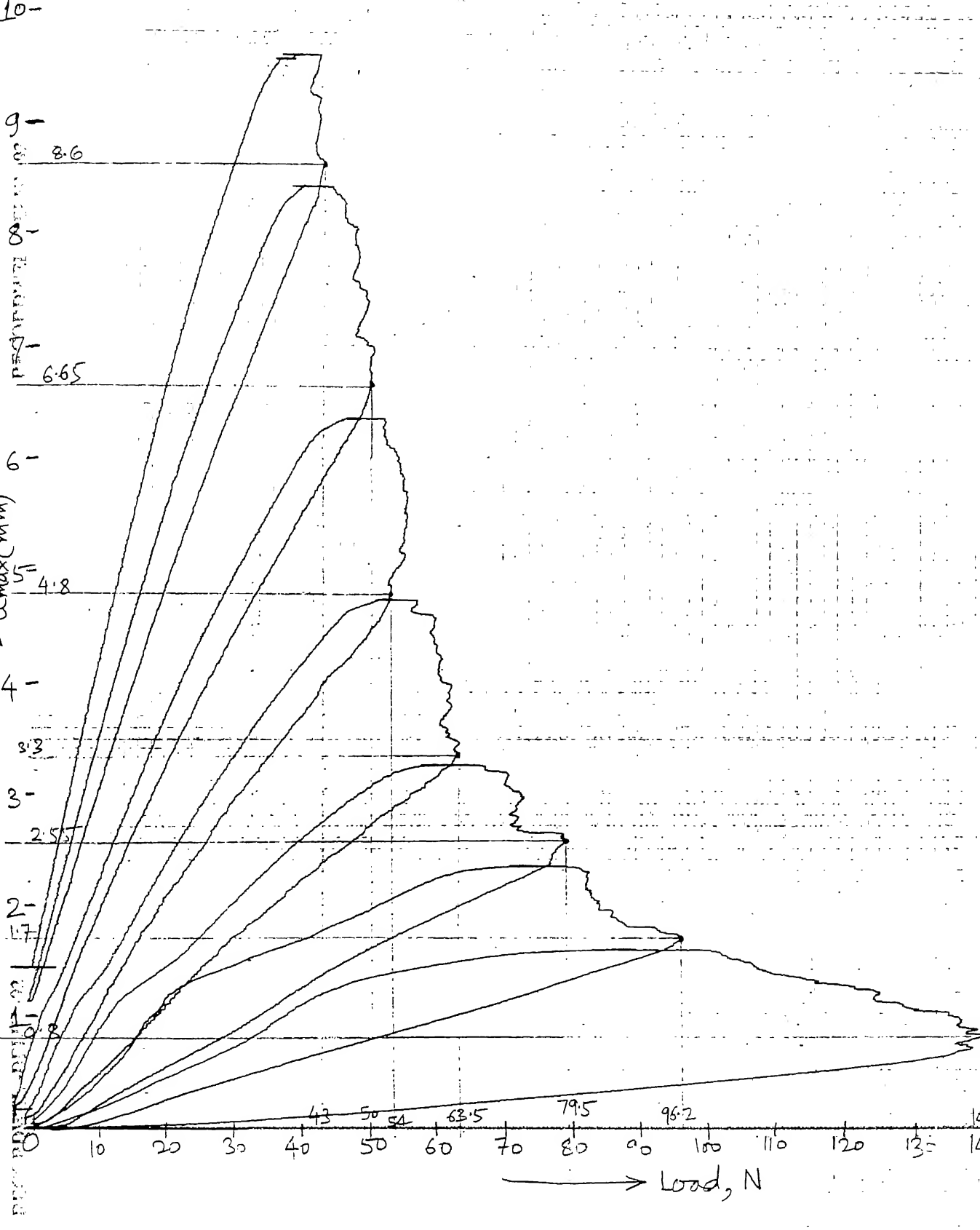

Fig.5.15 Critical Load vs. Displacement graph of DCB specimen (Exp-3)

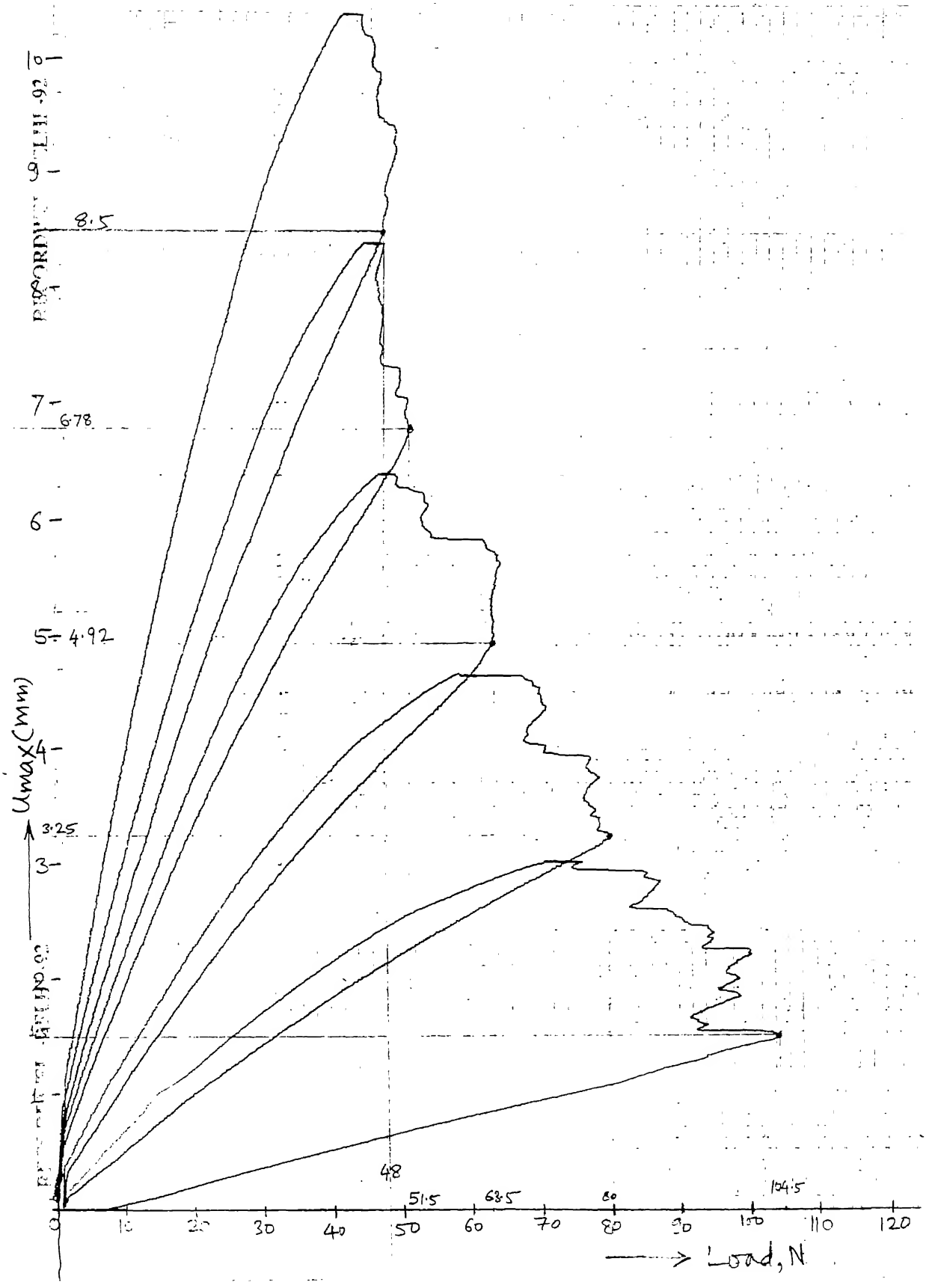

Fig.5.16 Critical Load vs. Displacement graph of DCB specimen(Exp-4)

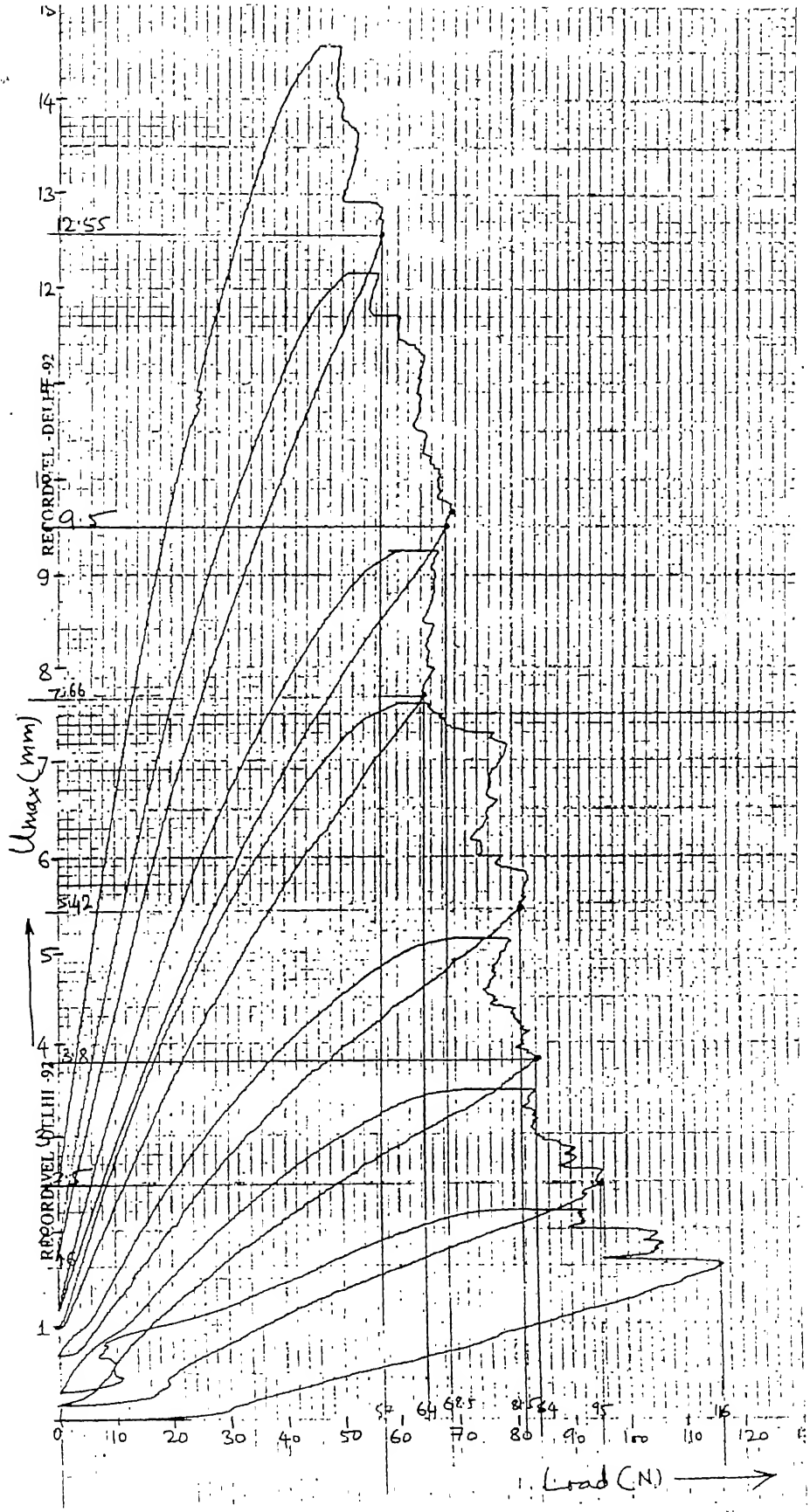

Fig.5.17 Critical Load vs. Displacement graph of DCB specimen (Exp-5)

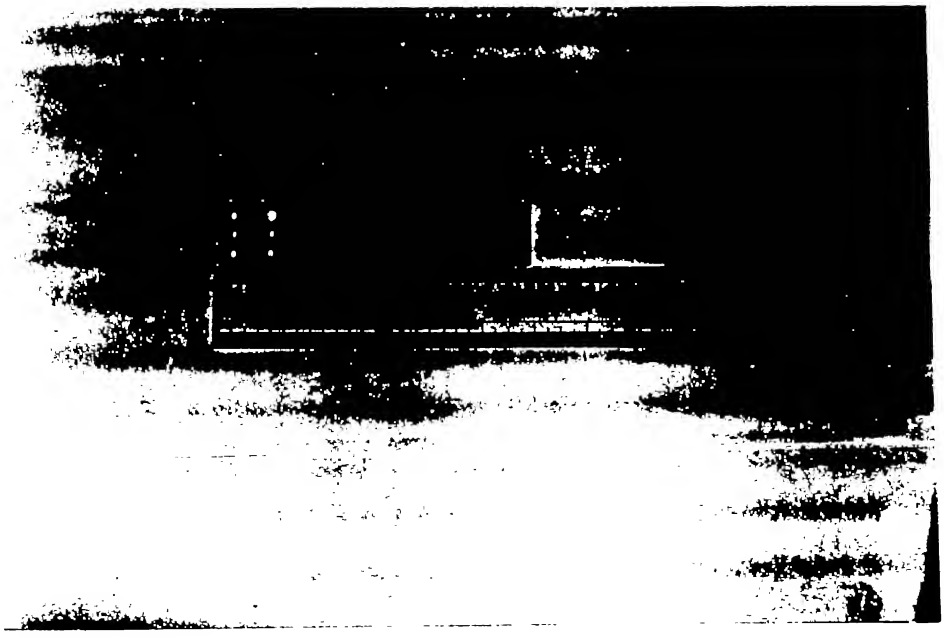

Fig.5.18 Photograph showing DCB specimen with crack fronts

CHAPTER-6

CONCLUSION

6.1 CONCLUSION

An experimental technique is developed by Kumar & Reddy, 1997, to determine Interlaminar Fracture Toughness (G_{Ic}) of isotropic materials by Embedded Crack Plate (ECP) specimen. This idea has been extended to composites, which has close resemblance of crack growth during impact.

For analysis of ECP specimens of composites, we have moved to experimental-numerical technique because analytical closed form solutions are not available due to elliptical crack profiles obtained. In the initial stage of the work, numerical technique to determine G_I has been developed and validated with closed form solutions available. It has been found that results obtained match closely within 9% of deviation.

The numerical technique is then applied to the experimentally obtained data for composites. The three types of composite laminates have been analysed. The results obtained with ECP specimen of glass fabric/epoxy laminate of sequence $[0]_{32}$ is compared with the DCB specimen of same laminate. It has been observed that G_{Ic} obtained through ECP specimen in 0° and 90° directions are considerably less than that of DCB specimens of $[0]_{32}$ and $[90]_{32}$ configurations. Thus, a designer is on the safe side if fracture toughness of composite is determined through ECP specimen.

6.2 SUGGESTIONS FOR FUTURE WORK

(1) Experimental setup should be improved by drilling a through hole in the CSK screw to accommodate a dowel pin during curing. After curing, this dowel pin should be removed.

(2) Before loading the specimen in the tensile testing machine a small diameter hole should be drilled near the centre to remove vacuum created inside the specimen.

(3) In glass fiber/epoxy laminate of $[0/90]_{8s}$ configuration, crack shifts the plane through transverse cracking. This should be accounted during FEM analysis.

(4) The ECP specimen technique should be extended to dynamic loading to model real life impact problems.

(5) The mesh should be further refined to get good results.

REFERENCES

Agarwal B.D and Broutman L.J., 1990, "Analysis and Performance of Fibre Composites", Second edition, John Wiley & Sons.

Albersten H., Ivens J., Peter P., Wevers M. and Verpoest I., 1995, "Interlaminar Fracture Toughness of CFRP influenced by Fiber Surface Treatment: Part 1. Experimental Results", Composite Science and Technology, Vol.54, PP.133-145.

Bascom W.D., Bitner J.L., Moulton R.J. and Siebert A.R., 1980, "The Interlaminar Fracture of Organic Matrix Woven Reinforcement Composites", Composites, Vol.11, No.1, PP.9-18.

Bathe Klauss-jurgen (1990), Finite Element procedures in Engineering Analysis, Prentice Hall of India.

Baumeister.T and Marks. L.S., 1958, "Standard Hand Book for Mechanical Engineers", Seventh edition, Mc Graw-Hill.

Bazhenov S.L., 1990, "Strong Bending in the DCB Interlaminar Test of thin E-Glass woven -fabric Reinforced Laminates', Composites, Vol.22. No.4, PP 275-280.

Bazhenov S.L., 1995, "Interlaminar and Intralaminar Fracture modes in 0/90 cross-ply Glass/Epoxy Laminate", Composites, Vol.26, No.2, PP.125-133.

Broek D., 1984, Elementary Engineering Fracture Mechanics", Martin-sus Nijhoff publishers.

Cook Robert D., Malkus, David S. and Plesha Micheal E., 1989, "Concepts and Applications of Finite Element Analysis", 3rd edition, John Wiley and Sons, NewYork.

Davies P., Moulin C., Kausch H. and Fischer M., 1990, "Measurements of G_{Ic} and G_{IIc} in Carbon/Epoxy Composites", Composite Science and Technology, Vol. 39, PP.193-205.

Devitt D.F., Schapery R.A. and Bradly W.L., 1980, " A Method for determining the Mode I Fracture of Elastic and Viscoelastic Composite Materials", Journal of Composite Materials, Vol.14, No.4, PP.270-285.

Doxsee L.E., Rubrecht P., Li L. and Verpoest.I, 1993, "Delamination Growth in Composite Plates subjected to Transverse Loads", Journal of Composite Materials, Vol. 27, No.8, PP.764-781.

Falzon B.G., Hitchings D. & Besant T., 1999, "Fracture Mechanics using 3D Composite Elements", Composite Structures, Vol.45, PP.29-39.

Irwin.G.R , 1957, "Relation of Stress near a Crack to the Crack Extension Force", 9 th Int. Congr. Appl. Mech., Vol.8, PP.245-251.

Irwin. G.R.1957, "Analysis of Stresses and Strains near the end of a Crack Traversing a Plate", J. Appl. Mech. Vol 24, PP 361-364.

Jagannadha Rao.,1997, "Experimental determination of Interlaminar Toughness in FRP Laminates using a Fully Embedded Crack", M.Tech Thesis,Mech Engg, IIT,Kanpur.

Joon-Hyung Byun., John Gillepsie,Jr . and Tsu-wei-chou,1990, "Mode I Delamination of 3-D Fabric Composite", Journal of Composite Materials, Vol 24 , PP 497-518.

Keary P.E., Ilcewicz L.B., Shaar C. and Trostle J., 1986, " Mode I Interlaminar Fracture Toughness of Composites using Slender Double Cantilever Beam Specimen", Journal of Composite Materials, Vol.39,No.2, PP.154-177.

Khalil A.A and Bayouni M.R.,1991, "Effect of Loading Rate on Fracture Toughness of Bonded Joints', Engineering Fracture Mechanics, Vol.39, No.6, PP.1037-1043.

Kumar. P., 1993 , "A Special Laminate for determining Interlaminar G_{Ic} ", NASAS 1993, Proceedings of National Seminar on Aerostructures, PP.79-90,IIT Kanpur.

Kumar. P.and Reddy .S.R. 1997," Experimental determination of Interlaminar Fracture Toughness in Plexiglass Plate with Fully Embedded Crack", Engineering Fracture Mechanics.

Kumar. P., Goel.B and Bandyopadhyay.J, 1995, "Unidirectional Prepreg Machine-An indigenous development ", IE(I) Journal -AS, Vol.75, No.3,PP 6-9.

Kumar.P., 1999, "Elements of Fracture Mechanics", Wheeler Publishing, New Delhi.

Kyung S.Han and James Koutsky., 1981, " The Interlaminar Fracture Energy of Glass Fibre Reinforced Polyster Composites", Journal of Composite Materials,Vol. 15, PP.371-388.

Pagano N.J. and Pipes R.B.,1971, " The Influence of Stacking Sequence on Laminar Strength", Journal of Composite Materials, Vol.5 PP.50-75.

Rajkumar B., 1998, "An Experimental-Numerical Technique to determine Interlaminar Fracture Toughness through an Embedded Crack Plate specimen", M.Tech Thesis Mechanical Engg. Dept., IIT Kanpur.

Raju. I.S., 1987, " Calculation of Strain Energy Release Rate with Higher Order and Singular Finite Elements", Engineering Fracture Mechanics, Vol 28, PP 251-274

Reddy J.N., 1993, "An Introduction to the Finite Element Method ", 2nd Ed., McGraw – Hill, Inc.

Ramakrishna. A.,1997, " Initiation and Propagation Toughness of Interlaminar Cracks in GFRP Laminates under Impact Loading, M.Tech Thesis, Mech Engg, IIT.Kanpur.

Reddy.,1996, "A New Technique to determine Interlaminar Fracture Toughness through a Penny Crack", M.Tech thesis, Mech Engg ,IIT, Kanpur.

Rybicki. E.F and Kanninen. M.F .,1977, " A Finite Element Calculation of Stress Intensity Factors by a Modified Crack Closure Integral", Engineering Fracture Mechanics, Vol. 9, PP 931-938.

Rybicki.E.F., Schmueser D W. and Fox.J.,1977, " An Energy Release Rate approach for Stable Crack growth in Free Edge Delamination problem", Journal of Composite Materials, Vol.11, PP.470-487.

Sarkar.P.K. and Maiti.S.K.,1991, "Prediction of Mode I Fracture Toughness of a Laminated Fibre Composite from Matrix Fracture Toughness of basic layer", Engineering Fracture Mechanics, Vol.33, No.1, PP.71-82.

Lee.S.M., 1996, "A comparison of Fracture Toughness of Matrix Controlled Fracture behaviour", Composite Science & Technology, Vol.43, PP 317-327.

Timoshenko. S.P. and Woinowsky. K.S, 1959, 'Theory of Plates' and Shells ", Second edition ,Mc-Graw Hill Int Edn.

Users Manual for FEMAP Version-5.0.

Users Manual for CSA/NASTRAN, 1994, Computerised Structural Analysis & Research Carporation, USA.

Wang.S.S., 1983, "Fracture Mechanics for Delamination Problems in Composite Materials, Vol.17, PP 210-223.

Wang.Y and Hao.D., 1995 " Characterization of Interlaminar Fracture behavior of Woven Fabric Reinforced Polymeric Composites", Composites, Vol.26 PP.115-124.

Young W.C., 1989, "Roark's Formulas for Stress and Strain", 6th Ed., McGraw – Hill Book Company, New Yark.

APPENDIX-A

Regression Analysis

Data analysis for finding G_{IC} requires fitting of a line of known slope to experimentally obtained data. A typical Load-Displacement curve that can be obtained from DCB specimen is shown in Fig. . For each crack length, corresponding compliance from the loading part of the graph and corresponding critical load are noted down.

Taking logarithm of Eq.(2.16),

$$\ln C = \ln A_1 + 3 \cdot \ln a.$$

From this equation, it is clear that (lnC) Vs (lna) plot should give a straight line with a slope 3. Therefore, a straight line with slope 3 fitted to the experimentally obtained data, yields $\ln A_1$ as the cut-off ordinate by the straight line.

Now similarly taking logarithm of Eq.(2.18),

$$\ln P_c = \ln A_2 - \ln a.$$

In a similar fashion a straight line fitted with -1 slope to the experiment data yields the constant A_2. In the present work, to determine A_1 & A_2, we are using linear regression method given by:

$$\ln A_1 = \frac{1}{n}\sum_{i=1}^{n}(\ln C - 3\ln a)$$

and,

$$\ln A_2 = \frac{1}{n}\sum_{i=1}^{n}(\ln P_c + \ln a).$$

By knowing A_1 & A_2, we can calculate Energy Release Rate using:

$$G_{IC} = \frac{3}{2}\frac{A_1 A_2^2}{b}.$$